PLOS ONE

RESEARCH ARTICLE

Mini-G proteins: Novel tools for studying GPCRs in their active conformation

Rony Nehmé[1], Byron Carpenter[1¤], Ankita Singhal[1], Annette Strege[1], Patricia C. Edwards[1], Courtney F. White[2], Haijuan Du[2], Reinhard Grisshammer[2], Christopher G. Tate[1]*

1 MRC Laboratory of Molecular Biology, Cambridge, United Kingdom, **2** Membrane Protein Structure Function Unit, National Institute of Neurological Disorders and Stroke, National Institutes of Health, Department of Health and Human Services, Rockville, United States of America

¤ Current address: Warwick Integrative Synthetic Biology Centre, School of Life Sciences, Gibbet Hill Campus, University of Warwick, Warwick, United Kingdom
* cgt@mrc-lmb.cam.ac.uk

Citation: Nehmé R, Carpenter B, Singhal A, Strege A, Edwards PC, White CF, et al. (2017) Mini-G proteins: Novel tools for studying GPCRs in their active conformation. PLoS ONE 12(4): e0175642. https://doi.org/10.1371/journal.pone.0175642

Editor: Arun Shukla, Indian Institute of Technology Kanpur, INDIA

Received: February 2, 2017

Accepted: March 29, 2017

Published: April 20, 2017

Data Availability Statement: All relevant data are within the paper and its Supporting Information files.

Funding: This research was supported by the European Research Council (EMPSI 339995; R.N., A.S., C.G.T.), Heptares Therapeutics (B.C., C.G.T.), the Medical Research Council (MC_U105197215; A.S., P.E., C.G.T.) and the Intramural Research Program of the National Institutes of Health, National Institute of Neurological Disorders and Stroke (ZIA NS003016-11; C.F.W., H.D., R.G.). The funders had no role in study design, data collection

Abstract

Mini-G proteins are the engineered GTPase domains of Gα subunits. They couple to GPCRs and recapitulate the increase in agonist affinity observed upon coupling of a native heterotrimeric G protein. Given the small size and stability of mini-G proteins, and their ease of expression and purification, they are ideal for biophysical studies of GPCRs in their fully active state. The first mini-G protein developed was mini-G_s. Here we extend the family of mini-G proteins to include mini-G_{olf}, mini-G_{i1}, mini-G_{o1} and the chimeras mini-$G_{s/q}$ and mini-$G_{s/i}$. The mini-G proteins were shown to couple to relevant GPCRs and to form stable complexes with purified receptors that could be purified by size exclusion chromatography. Agonist-bound GPCRs coupled to a mini-G protein showed higher thermal stability compared to the agonist-bound receptor alone. Fusion of GFP at the N-terminus of mini-G proteins allowed receptor coupling to be monitored by fluorescence-detection size exclusion chromatography (FSEC) and, in a separate assay, the affinity of mini-G protein binding to detergent-solubilised receptors was determined. This work provides the foundation for the development of any mini-G protein and, ultimately, for the structure determination of GPCRs in a fully active state.

Introduction

G protein-coupled receptors (GPCRs) are integral membrane proteins that play a ubiquitous role in intercellular communication throughout the human body. Binding of an agonist at the extracellular surface of the inactive receptor results ultimately in a conformational change at its intracellular surface that allows G protein coupling [1]. The conformation of the bound G protein is altered around the nucleotide binding pocket, resulting in GDP release, binding of GTP and subsequent activation of the G protein [2]. There has been great progress in the structure determination of GPCRs in the inactive state [3] bound to antagonists which highlights common structural features of the GPCR superfamily [4], a common mode of activation [5] and a conserved mechanism for the activation of G proteins [6]. However, it is still a major challenge to determine the structures of receptors in their fully active state, which can be defined structurally as the conformation bound to a heterotrimeric G protein or pharmacologically as the high-affinity agonist

and analysis, decision to publish, or preparation of the manuscript.

Competing interests: CGT is a consultant, shareholder and member of the Scientific Advisory Board of Heptares Therapeutics. This does not alter our adherence to PLOS ONE policies on sharing data and materials. BC was also funded by a grant from Heptares Therapeutics.

binding state of the receptor. The range of GPCR structures now available allows a clear distinction between agonist-bound structures either in the inactive state [7–10], in an active-intermediate state [11–14] or in an active state [2, 15–20]. It is, however, difficult to determine structures of receptors in an active state due to the instability of activated GPCRs and receptor-bound G proteins.

Four solutions have been developed to determine the active structures of GPCRs. The first active structure determined was of opsin stabilized at low pH [21] and bound to a C-terminal fragment of the G protein transducin [22]. This methodology has not been successful for any other GPCR. The second active state structure of a GPCR was determined of the β_2-adrenergic receptor (β_2AR) bound to a single-chain camelid antibody (nanobody) that mimics the pharmacological effects of a heterotrimeric G protein [15]. This has been applied successfully to other GPCRs [18, 19], but currently the methodology still requires the immunization of llamas with purified receptors [23], which makes it difficult to apply to many unstable GPCRs. The third methodology was to crystallise β_2AR with the entire heterotrimeric G protein [2]. This was a great achievement and showed for the first time how a GPCR facilitated nucleotide exchange in the G protein. However, no other structures of a GPCR coupled to a heterotrimeric G protein have been published and the resolution of the GPCR portion of the structure was poor and required the previously determined active state structure of β_2AR bound to a nanobody to allow the model to be built [2]. The fourth methodology was based on the observation that only the GTPase domain of the Gα subunit made significant contacts with active β_2AR and therefore this domain was engineered and thermostabilised to generate a mini-G protein, mini-G_s [24]. Like the nanobodies, mini-G_s recapitulated all the receptor pharmacology upon coupling, but in addition, mini-G_s could couple to any G_s-coupled receptor whereas nanobodies bound to only a specific receptor. The structure of the adenosine A_{2A} receptor (A_{2A}R) coupled to mini-G_s was determined recently [20], which showed similar structural rearrangements observed in the β_2AR–G_s complex.

The concept of mini-G proteins shows great promise for accelerating the rate of structure determination of GPCRs in their active states, from providing biophysical and pharmacological data on receptors in the active state, as well as providing a potential binding partner in co-crystallisation applications. However, there are four families of Gα subunits (Fig 1; $G\alpha_s$, $G\alpha_i$, $G\alpha_q$, and $G\alpha_{12}$) that show different specificities for various GPCRs [25]. Thus to be truly useful as tools in structural biology, at least one member from each family needs to be converted into a mini-G protein. Here we report the development of mini-G proteins for all the major Gα families. We also describe five different assays that can be used to characterize the binding of the mini-G proteins to GPCRs and show in three cases that the complexes can be purified by size exclusion chromatography. The two different methodologies for generating the mini-G proteins can be applied easily to any other Gα subunit, opening the doorway to studies on potentially any GPCR from any species.

Materials and methods

Ligands

The β_1-adrenergic receptor (β_1AR) agonist isoproterenol hydrochloride and inverse agonist ICI118551 hydrochloride were from Sigma-Aldrich. The adenosine A_{2A} receptor (A_{2A}R) agonist NECA and antagonist ZM241385 were also from Sigma Aldrich. Serotonin $5HT_{1B}$ receptor ($5HT_{1B}$R) agonist donitriptan hydrochloride and selective antagonist SB224289 hydrochloride were from Santa Cruz Biotechnology; the agonist sumatriptan succinate was from Cayman chemical. Angiotensin II receptor (AT_1R) agonist angiotensin II was from Tocris. All radioactive ligands were from PerkinElmer.

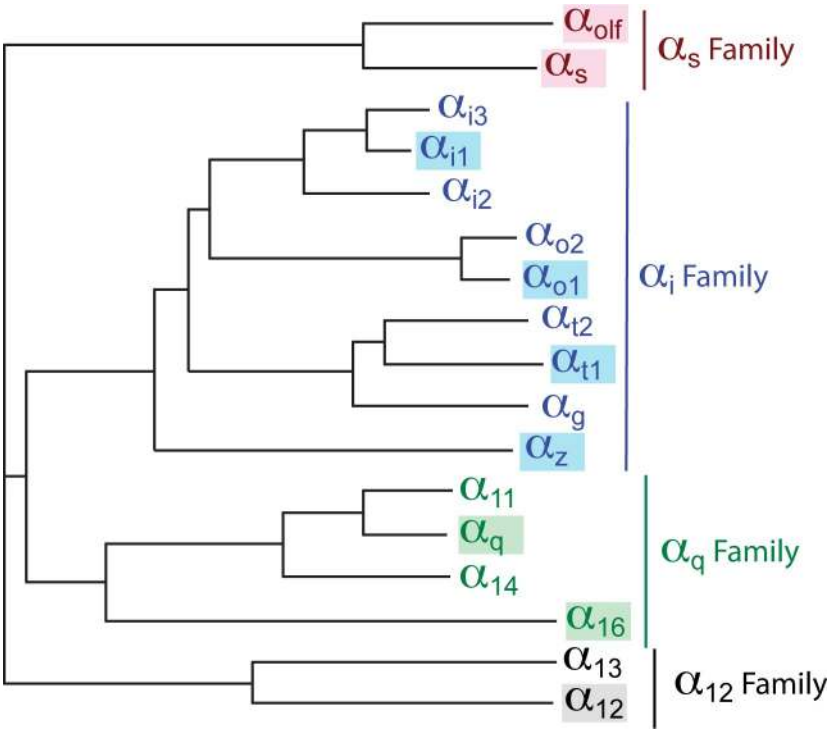

Fig 1. Phylogenetic relationship of human Gα subunits. All the Gα subunits that have been highlighted in the family-specific colours were attempted to be converted into mini-G proteins. The phylogenetic relationships were determined using TreeDyn.

https://doi.org/10.1371/journal.pone.0175642.g001

GPCR constructs, expression and purification

Human adenosine A_{2A} receptor ($A_{2a}R$). Two different $A_{2A}R$ constructs were used during this work. For SEC experiments using purified receptor, an $A_{2A}R$ construct was used that contained an N-terminal thioredoxin fusion protein to increase the molecular weight of the receptor. Without this fusion protein, $A_{2A}R$ and the mini-G protein had identical mobility on SDS-PAGE, thus making it difficult to visualise the separate components when analyzing a complex. The thioredoxin-$A_{2A}R$ fusion protein consisted of an N-terminal cleavable leader sequence (gp67), His10 tag and TEV protease cleavage site, followed by thioredoxin, which was connected to wild-type human $A_{2A}R$ (residues 6–316) through an EAAAKA linker. $A_{2A}R$ contained the N154A mutation to remove a potential N-linked glycosylation site. For all other experiments, a C-terminally truncated human $A_{2A}R$ construct was used (residues 1–317), which contained a C-terminal His10 tag and TEV protease cleavage site and the N154A mutation to remove the potential N-linked glycosylation site. Both constructs were expressed using the baculovirus expression system as described previously [20, 26]. Cells were harvested by centrifugation 72 hours post infection, resuspended in hypotonic buffer (20 mM HEPES pH7.5, 1 mM EDTA, 1 mM PMSF), flash-frozen in liquid nitrogen and stored at −80˚C until use. Purification of the receptor was performed in DDM using Ni^{2+}-affinity chromatography followed by SEC essentially as described previously [20, 26].

Turkey β_1-adrenergic receptor (β_1AR). A truncated version of wild type turkey β_1AR (construct βAR6; [27]) contained truncations at the N-terminus and the C-terminus and a C-terminal His6 tag for purification [27], and was expressed using the baculovirus expression system at 27˚C as described previously [28]. Cells were harvested by centrifugation 48 hours

post infection, resuspended in hypotonic buffer (20 mM Tris-HCl pH8, 1 mM EDTA, 1 mM PMSF), flash-frozen in liquid nitrogen and stored at -80˚C until use.

Human angiotensin type II receptor 1 (AT_1R). Wild type AT_1R (residues 1–359) had a C-terminal factor X cleavage site followed by GFP and a His10 tag for purification, and was expressed using the tetracycline-inducible mammalian expression system as a stable cell line in HEK293 cells [29]. Cells were grown in DMEM containing 5% tetracycline-free FBS until they were 80% confluent and then tetracycline was added to a final concentration of 1 μg/ml. Cells were grown for 24 hours and then harvested, and resuspended in PBS, flash frozen in liquid nitrogen and stored at -80˚C until use.

Rat neurotensin receptor (NTSR1). NTSR1 was expressed as described previously [13]. The baculovirus construct NTSR1 consisted of the hemagglutinin signal peptide and the Flag tag, followed by the wild-type rat NTSR1 (residues 43–396) and a C-terminal His10 tag. Recombinant baculovirus was generated using a modified pFastBac1 transfer plasmid (Invitrogen). *Trichoplusia ni* cells were infected with recombinant virus, and the temperature was lowered from 27˚C to 21˚C. Cells were harvested by centrifugation 48 hours post infection, resuspended in hypotonic buffer (10 mM HEPES pH 7.5, 10 mM $MgCl_2$, 20 mM KCl), flash-frozen in liquid nitrogen and stored at -80˚C until use.

Human serotonin $5HT_{1B}$ receptor ($5HT_{1B}R$). Wild-type $5HT_{1B}R$ (residues 34–390) was modified to contain a C-terminal TEV cleavage site and a His10 tag, cloned into plasmid pBacPAK8 and recombinant baculoviruses were prepared using the FlashBAC ULTRA system (Oxford Expression Technologies). *Trichoplusia ni* cells were grown in ESF921 media (Expression Systems) to a density of $3x10^6$ cells/ml, infected with $5HT_{1B}R$ baculovirus and incubated for 48 h at 27˚C for expression. Purification of the receptor was performed in either DDM or LMNG using Ni^{2+}-affinity chromatography followed by SEC.

Expression, purification and stability of G protein subunits

For constructs see Fig 2 and S1–S3 Figs. Expression, purification and stability measurements by differential scanning fluorimetry (DSF) of the mini-G proteins as well as the non-lipidated $G\beta_1\gamma_2$ dimer, were performed following the protocols described in [24, 30]. The stability of mini-G proteins was also determined in detergent using native DSF (NanoTemper Prometheus). Mini-G proteins (2 mg/ml) in 50 mM HEPES pH 7.5 (KOH), 20 mM $MgCl_2$, 50 mM NaCl, 1 μM GDP were mixed with either no detergent (control), 0.1% LMNG or 0.1% DDM. Samples were incubated on ice (minimum 30 min) prior to heating on the Prometheus (20% excitation, 15˚C-85˚C, rate of 2.0˚C/min) and the onset of scattering determined. The conditions used for the native DSF measurements mimic those used in the formation of a mini-G protein–GPCR complex (contains 1 μM GDP and detergent), which differ from the conditions used for good stability of the GDP-bound state of mini-G proteins (contains 1 mM GDP and no detergent).

SEC

(1) $A_{2A}R$–mini-G_s complex. The thioredoxin fusion construct of $A_{2A}R$ was purified in DDM essentially as described previously [19]. $A_{2A}R$ and mini-G protein were mixed in a 1:1.2 molar ratio, apyrase (0.1 U/ml final concentration) was added and the sample was incubated overnight on ice before loading onto a Superdex S200 10/300 size exclusion column (10 mM HEPES pH 7.5, 100 mM NaCl, 1 mM $MgCl_2$, 100 μM NECA, 0.02% DDM; 4˚C, 0.5 ml/min). Peak fractions were analysed by SDS-PAGE.

(2) $5HT_{1B}R$–mini-G_{o1} complex. Donitriptan-bound $5HT_{1B}R$ purified in DDM was mixed with mini-G_{o1} in a 1:1.2 molar ratio. Apyrase (0.1 U/ml final concentration) was added

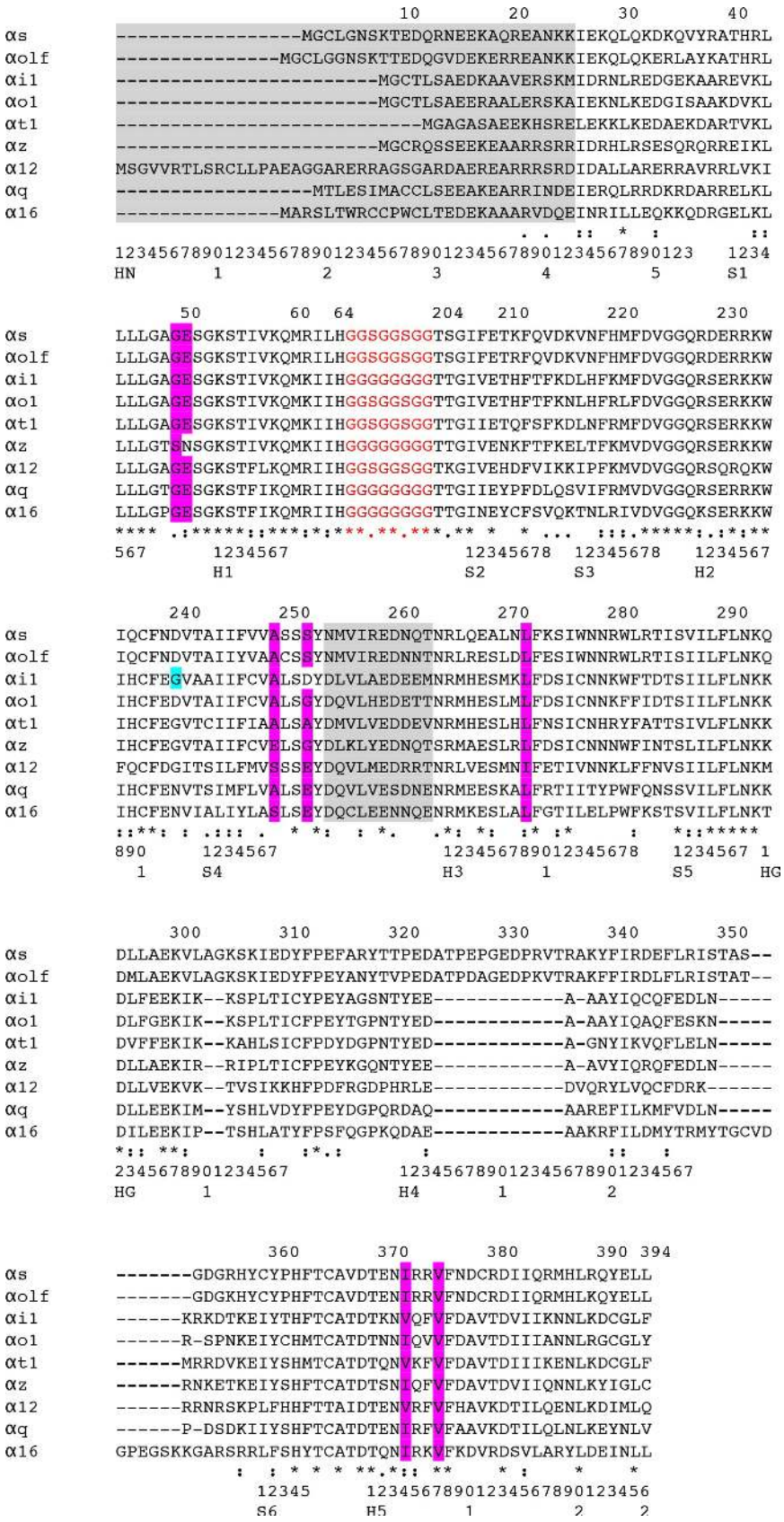
αs
αolf
αi1
αo1
αt1
αz
α12
αq
α16
HN 1 2 3 4 5 S1
S1 H1 S2 S3 H2
H2 S4 H3 1 S5 HG
HG 1 H4 1 2
S6 H5 1 2 2

Fig 2. Alignment of Gα GTPase domain protein sequences. The amino acid sequences aligned are of the wild type GTPase domains of the Gα subunits used in this study to create the initial mini-G proteins. The GαAH domain (not shown) was deleted and replaced by a linker (GGGGGGGG or GGSGGSGG in red). To construct mini-G proteins, the residues highlighted in grey were deleted and residues highlighted in magenta were mutated to the following ($G\alpha_s$ residue number and the CGN in superscript): $D49^{S1H1.3}$, $N50^{S1H1.4}$, $D249^{S4.7}$, $D252^{S4H3.3}$, $D272^{H3.8}$, $A372^{H5.4}$, $I375^{H5.7}$. The glycine mutation (G217D, highlighted in cyan) was incorporated into G_{i1} only, to improve expression (see Results & Discussion). Numbering above the sequences is for $G\alpha_s$ and the CGN system below the sequence is used for reference [6].

https://doi.org/10.1371/journal.pone.0175642.g002

and the sample was incubated 4 h on ice before loading onto a Superdex S200 10/300 size exclusion column (20 mM HEPES pH 7.5, 100 mM NaCl, 1 mM $MgCl_2$, 1 μM donitriptan, 0.03% DDM; 4˚C, 0.5 ml/min). Peak fractions were analysed by SDS-PAGE.

FSEC assays

(1) $A_{2A}R$. Insect cell membranes containing a total of 20 μg (560 pmol) wild-type $A_{2A}R$ (20 x 10^6 cells) were solubilized for 30 min on ice in 40 mM HEPES pH7.5, 500 mM NaCl, 2 mM $MgCl_2$, 2 U/mL apyrase (Sigma-Aldrich), and 0.5% (v/v) DDM (final volume of 2 ml, concentration of $A_{2A}R$ 280 nM). Insoluble material was removed by ultracentrifugation (30 min, 4˚C, 135,000 x*g*). The supernatant was divided into aliquots for the subsequent assay. To 900 μl of the supernatant was added either the agonist NECA or the inverse agonist ZM241385 (negative control), both at a final concentration of 60 μM. GFP-mini-G_s (6 μg; 110 pmol, final concentration 122 nM) was then added and allowed to bind for 90 min on ice before loading 200 μl onto a Superdex S200 10/300 size exclusion column (buffer 20 mM HEPES pH 7.5, 100 mM NaCl, 10 mM $MgCl_2$, 1 μM NECA or ZM241385, 0.03% DDM, 4˚C, flow rate 0.45 ml/min). The control sample contained 6 μg GFP-mini-G_s only in 500 μl assay buffer. GFP fluorescence was detected by a Hitachi fluorometer (mV) set to an excitation of 488 nm and an emission of 525 nm.

(2) β_1AR. Insect cell membranes containing a total of 8 μg (178 pmol) wild-type β_1AR (30 x 10^6 cells) were solubilized for 30 min on ice in 20 mM Tris-HCl pH8, 500 mM NaCl, 5 mM $MgCl_2$, 2 U/mL apyrase and 0.5% (v/v) DDM (final volume 2 ml, β_1AR concentration 90 nM). Insoluble material was removed by ultracentrifugation (30 min, 4˚C, 135,000 x*g*). The supernatant was divided into aliquots for the subsequent assay. Isoprenaline (100 μM final concentration) or ICI118551 (10 μM final concentration) were added to 500 μl of the supernatant. GFP-mini-G_s (6 μg, 110 pmol) was then added to give a final concentration of 122 nM and allowed to bind for 90 min on ice before loading 200 μl onto a Superdex S200 10/300 size exclusion column (buffer 20 mM HEPES pH 7.5, 100 mM NaCl, 10 mM $MgCl_2$, 1 μM isoprenaline or ICI118551, 0.03% DDM, 4˚C, flow rate 0.45 ml/min). The control sample contained 6 μg GFP-mini-G_s only in 500 μl assay buffer.

(3) $5HT_{1B}R$. When detergent-solubilized unpurified receptor was used, insect cells expressing 610 pmol $5HT_{1B}R$ (40 x 10^6 cells) were resuspended in 20 mM HEPES pH 7.5, 100 mM NaCl, 10 mM $MgCl_2$, 2 U/ml apyrase to a final cell density of 20 x 10^6 cells/ml and solubilized with 0.5% DDM (45 min, 4˚C, final volume 2 ml, $5HT_{1B}R$ concentration 305 nM). Insoluble material was removed by ultracentrifugation (30 min, 4˚C, 135,000 x*g*). The supernatant was divided into 900 μl aliquots for the subsequent assay. GFP-mini-G_{o1} (5 μg, 100 pmol) was added (final concentration 111 nM) with either donitriptan or SB224289, each to a final concentration of 100 μM, and allowed to bind for 90 min on ice before loading 500 μl onto a Superdex S200 10/300 size exclusion column. The control sample contained 5 μg GFP-mini-G_{o1} in 500 μl assay buffer.

In some FSEC experiments, purified $5HT_{1B}R$ was used. Donitriptan-bound, purified receptor (120 μg; 3 nmol) in either LMNG or DDM was incubated for 90 min on ice with 4 μg (60–80 pmol) either of GFP-mini-G_{i1}, GFP-mini-G_{o1} or GFP-mini-G_s (negative control) in a final

volume of 450 μl. Samples (200 μl) were then loaded onto Superdex S200 10/300 size exclusion column (buffer 20 mM HEPES pH 7.5, 100 mM NaCl, 10 mM $MgCl_2$, 1 μM donitriptan, 0.03% DDM or 0.001% LMNG buffer, 4˚C, flow rate 0.45 ml/min). The final concentration of purified $5HT_{1B}R$ was 6.7 μM and the final concentrations of the mini-G proteins were as follows: GFP-mini-$G_{s/i1}$, 133 nM; GFP-mini-G_{i1}, 167 nM; GFP-mini-G_{o1}, 170 nM; GFP-mini-G_s, 167 nM; GFP-mini-$G_{i1}\beta_1\gamma_2$, 90 nM.

Fluorescent saturation binding assay (FSBA)

(1) β_1AR. Membranes prepared from insect cells expressing β_1AR (50 x 10^6 cells) were solubilized in 20 mM Tris-HCl pH8, 500 mM NaCl, 3 mM imidazole, 2 U/ml apyrase 0.5% DDM (1 hour, 4˚C, final volume 8 ml, β_1AR concentration 37.5 nM). Insoluble material was removed by ultracentrifugation (30 min, 4˚C, 135,000 x*g*) and the supernatant was divided into two aliquots. The agonist isoprenaline was added to one sample (final concentration 10 μM) and the inverse agonist ICI118551 was added to the other (final concentration 1 μM). Samples were then aliquoted 200 μl per well into a black Ni^{2+}-coated 96-well plate (Pierce; Thermo Fisher). The receptor was allowed to bind *via* its His tag for 1 h on ice. The supernatant was then aspirated and 200 μl GFP-mini-G_s at varying concentrations (0 to 2.8 μM) were added and incubated for a further 90 min on ice. The supernatant was then removed by aspiration and each well washed 4 times with buffer A (10 μM isoprenaline (agonist), 20 mM Tris-HCl pH8, 100 mM NaCl, 1 mM $MgCl_2$, 1 mg/mL BSA, 30 mM imidazole, 0.03% DDM,) or buffer B (1 μM ICI118551 (inverse agonist), 20 mM Tris-HCl pH8, 100 mM NaCl, 1 mM $MgCl_2$, 1 mg/mL BSA, 30 mM imidazole, 0.03% DDM). Elution of the receptor–GFP-mini-G_s complex from the sides of the well to make a homogeneous solution was performed with 200 μl of the respective wash buffers that contained 300 mM imidazole. Fluorescence was then measured using a Pherastar plate reader (BMG Labtech, Inc.) with excitation at 485 nm and emission at 520 nm. ΔF data (fluorescence agonist condition minus fluorescence antagonist condition) corresponding to specific binding were analysed by non-linear regression using GraphPad Prism version 5.0 (GraphPad Software, San Diego, CA) and apparent K_D values derived from one site-specific binding analysis.

(2) A_{2A}R. The assay was performed essentially as described above for β_1AR, but the buffer conditions were different. Solubilisation of insect cell membranes (40 x 10^6 cells) was performed in 10 ml of 20 mM Tris-HCl pH8, 500 mM NaCl, 10 mM imidazole, 2 U/ml apyrase and 0.5% DDM (1 h, 4˚C, final volume 10 ml, A_{2A}R concentration 112 nM). After ultracentrifugation, the agonist NECA (10 μM final concentration) was added to one supernatant sample and the inverse agonist ZM241385 (10 μM final concentration) to the other. Washing buffers for A_{2A}R were buffer C (10 μM NECA, 20 mM Tris-HCl pH8, 100 mM NaCl, 1 mM $MgCl_2$, 1 mg/mL BSA, 50 mM imidazole, 0.03% DDM) or buffer D (10 μM ZM241385, 20 mM Tris-HCl pH8, 100 mM NaCl, 1 mM $MgCl_2$, 1 mg/mL BSA, 50 mM imidazole, 0.03% DDM).

(3) $5HT_{1B}$R. Insect cells expressing $5HT_{1B}$R (50 x 10^6 cells) were solubilized with buffer containing 10 μM Donitriptan, 20 mM Tris-HCl pH8; 500 mM NaCl; 10 mM imidazole, 2 U/ml apyrase and 0.5% DDM (1 h, 4˚C, final volume 6 ml, $5HT_{1B}$R concentration 127 nM). Insoluble material was removed by ultracentrifugation (30 min, 4˚C, 135,000 x*g*) and 200 μl of supernatant was then aliquoted per well into a black Ni^{2+}-coated 96-well plate. The receptor was allowed to bind *via* its His tag for 1 h on ice. The supernatant was then aspirated and 200 μl either of GFP-mini-$G_{o1,}$ GFP-mini-$G_{s/i1}$ or GFP-mini-G_s (negative control) at varying concentrations (from 0 to 5 μM) were added and incubated for a further 90 min on ice. The supernatant was then removed by aspiration and each well washed 4 times with buffer E (1 μM Donitriptan, 20 mM Tris-HCl pH8, 100 mM NaCl, 1 mM $MgCl_2$, 1 mg/mL BSA, 50 mM imidazole, 0.03% DDM).

Elution was carried out with 200 μL of buffer E containing 300 mM imidazole. ΔF data (fluorescence G_{o1} condition minus fluorescence G_s condition) corresponding to specific binding were analysed by non-linear regression using GraphPad Prism version 5.0 (GraphPad Software, San Diego, CA) and apparent K_D values derived from one site-specific binding analysis.

Competition binding assay

Insect cells expressing $5HT_{1B}R$ were resuspended in 1 ml of assay buffer (20 mM HEPES pH7.5, 100 mM NaCl, 1 mM $MgCl_2$, 1 mM ascorbate, 20 μM pargyline) at a final concentration of 2 x 10^6 cells/ml. Cells were sheared by 10 passages through a bent 26G needle. The supernatant was diluted 10-fold in assay buffer and aliquots (900 μl) taken for each sample. Mini-G protein (100 μl, 25 μM final concentration) or buffer (negative control) was added. The mixture was aliquoted into a 0.2 ml PCR plate, 96 μl per well. Sumatriptan (12 μl), prepared in assay buffer also containing 2 U/ml apyrase, was added to each well (final concentrations in the range of 100 pM to 1 mM). Non-specific binding was determined in the presence of 100 μM donitriptan. Samples were mixed and incubated at 4˚C for 2 h. [^{3}H]-GR125743 (12 μl) was added at its apparent K_D (10 nM) concentration. Samples were mixed and incubated at 4˚C for 2 h before filtering through 96-well glass fibre GF/B filter plate (Merck Millipore) and washing with ice-cold assay buffer. Filters were dried, punched into scintillation vials and 4 ml Ultima Gold scintillant (Perkin Elmer) were added. Radioactivity was quantified by scintillation counting (1 min per sample) using a Tri-Carb counter (Perkin Elmer), and K_i values were determined using GraphPad Prism version 5.0 (GraphPad Software, San Diego, CA)

Thermostability assay

(1) $A_{2A}R$. Membranes from *Trichoplusia ni* cells expressing wild-type human $A_{2A}R$ were resuspended in T_m buffer (25 mM HEPES pH 7.5, 100 mM NaCl, 1 mM $MgCl_2$) and homogenized by ten passages through a 26G needle. Mini-G protein was added at a final concentration of 25 μM. ^{3}H-NECA and unlabeled NECA, prepared in assay buffer containing 2 U/ml apyrase, were mixed in a molar ratio of 1:5 and added to the membranes to give a final concentration of 1 μM (approximately ten-fold above the apparent K_D). The samples were incubated at room temperature for 1 h, then chilled on ice for 30 min. Decylmaltoside (DM) was added to a final concentration of 0.13%, and samples were incubated on ice for 1 h. Cell debris and insoluble material were removed by centrifugation (5 min, 20,000 x*g*, 4˚C) and the supernatant was aliquoted (120 μl) into PCR strips. Samples were heated to the desired temperature for exactly 30 min, then quenched on ice for 30 min. Samples (50 μl) were loaded onto gel-filtration resin (Toyopearl HW-40F) packed into a 96-well filter plate (Millipore), which was centrifuged to separate receptor-bound from free radioligand [31]. Nonspecific binding was determined in the presence of 200 μM unlabelled NECA. Radioactivity was quantified by liquid scintillation counting using a MicroBeta TriLux scintillation counter (PerkinElmer). Data were analysed by nonlinear regression using GraphPad Prism software. Apparent T_m values were derived from sigmoidal dose-response analysis performed by non-liner regression. Results represent the mean ± SEM of two independent experiments, performed in duplicate.

(2) NTSR1. Cell pellets from 10 ml of insect cell cultures were resuspended in 1.8 ml buffer containing DDM to give a final buffer composition of 50 mM Tris-HCl pH 7.4, 100 mM NaCl, 1 mM MgCl2, 1% (w/v) DDM. The samples were placed on a rotating mixer at 4˚C for 1 hour. Cell debris and non-solubilized material were removed by ultracentrifugation (152,800 x*g*, 4˚C, 30 min), and the supernatant containing detergent-solubilized NTSR1 was used to test for thermal stability in the presence of NTS and mini-G proteins. For thermal denaturation

curves, the supernatants were diluted 6.67-fold into assay buffer (50 mM Tris-HCl pH 7.4, 100 mM NaCl, 1 mM $MgCl_2$) containing 22.5 μM mini-G protein and 10 nM ^{3}H-NTS and incubated for 1 hour on ice. After addition of apyrase (0.25 units/ml, NEB), the sample was placed on ice for an additional 30 min. Samples (120 μl aliquots) were exposed to different temperatures between 0˚C and 60˚C for 30 min and placed on ice. Separation of receptor–ligand–mini-G protein complex from free ^{3}H-NTS (100 μl) was achieved by centrifugation-assisted gel filtration (spin assay) using Bio-Spin 30 Tris columns (BioRad), equilibrated with RDB buffer [50 mM Tris-HCl pH7.4, 1 mM EDTA, 0.1% (w/v) DDM, 0.2% (w/v) CHAPS, 0.04% (w/v) CHS], essentially as described previously [32]. Control reactions on ice were recorded at the start and at the end of each denaturation experiment. The percentage of activity remaining after heat exposure was determined with respect to the unheated control. Data were analyzed by nonlinear regression using a Boltzmann sigmoidal equation in the Prism software (GraphPad).

(3) AT_1R. HEK 293 cells expressing wild type AT_1R were resuspended in a radioligand binding assay buffer (50 mM HEPES pH 7.4, 150 mM NaCl, 1 mM EDTA, 0.1% BSA, 40 μg/ml bacitracin) and homogenized by sonication (4 sec pulse). Mini-G protein and apyrase were added at a final concentration of 25 μM and 0.1 U/ml, respectively. ^{125}I-Ang II and unlabeled Ang II were added at a concentration of 0.5 nM and 25 nM respectively (approximately 50 times the apparent K_D value). The sample was incubated at room temperature (20˚C) for an hour, chilled on ice for 10 minutes and then digitonin was added to a final concentration of 1% and incubated on ice for an hour. Insoluble material was removed by centrifugation (2 min, 20,000 x*g*, 4˚C). The reaction mix was split into a number of 115 μl aliquots and each was incubated at various temperatures for exactly 30 minutes. The reactions were then quenched on ice for 5 minutes. ^{125}I-Ang II bound to AT_1R was separated from unbound ^{125}I-Ang II using centrifugation-assisted gel filtration column, essentially as described previously [29]. Non-specific binding was determined using a 500-fold excess of cold ligand. Radioactivity was measured using liquid scintillation counting. Data was analysed by non-linear regression using GraphPad prism software and apparent T_m values were derived by non-linear regression of the sigmoidal dose-response curve.

Results and discussion

Initial development of new mini-G proteins

The recently designed minimal G protein, mini-G_s [24], comprises only the GαGTPase domain from G_s and 3 deletions and 7 mutations to thermostabilise it (Fig 2). Mini-G_s coupled to both the β_1-adrenergic receptor (β_1AR) and the adenosine A_{2A} receptor (A_{2A}R), and resulted in the same increase in agonist affinity as observed for heterotrimeric G_s coupling [20, 24]. However, there are 4 families of Gα subunits (Fig 1) and GPCRs couple to distinct G proteins depending upon their physiological function [25]. Therefore, to provide tools for the structure determination of GPCRs in their fully active state, it was necessary to develop versions of mini-G proteins for at least one member from each of the other families. All of the mutations and deletions used to create mini-G_s are located within conserved regions of the Gα subunit (Fig 2). Therefore, in theory, these mutations were potentially transferable to the other Gα families, allowing the production of a panel of mini-G proteins capable of coupling to any GPCR.

Archetypical members from each Gα family were selected and include the following: G_{olf} from the G_s family, G_{i1}, G_{o1}, G_z and G_t from the G_i family, G_q and G_{16} from the $G_{q/11}$ family, and G_{12} from the $G_{12/13}$ family. The mutations required to convert $G\alpha_s$ into mini-G_s were transferred *en bloc* to the selected Gα proteins to produce a mini-G protein version of each (Fig 2). These mutations were the following: (i) deletion of all amino acid residues N-terminal of Ile/

Leu^{HN43}; (ii) deletion of the α-helical domain between residues H$^{H1S2.12}$ and the Thr, three residues N-terminal to Ile$^{S2.1}$, and replacement with an 8 amino acid residue linker; (iii) deletion of 10 amino acid residues of switch III between Tyr$^{S4H3.4}$ and Asn/Ser$^{S4H3.15}$; (iv) mutating 7 residues to D49$^{S1H1.3}$, N50$^{S1H1.4}$, D249$^{S4.7}$, D252$^{S4H3.3}$, D272$^{H3.8}$, A372$^{H5.4}$, I375$^{H5.7}$. Residue numbers are for Gα_s and superscripts refer to the CGN system for comparing residues in G proteins [6]. Initial characterization of each mini-G protein was performed by assessing expression in *Escherichia coli* and purification by Ni^{2+}-affinity chromatography and size exclusion chromatography (SEC). Four out of the eight engineered mini-G proteins (mini-G_{olf}, mini-G_{i1}, mini-G_{o1} and mini-G_{12}) fulfilled these initial criteria *i.e.* they were all stable enough in their basal conformation to allow high-yield expression and purification. The yield of purified mini-G protein per litre of culture and their stability as measured by differential scanning fluorimetry (in parentheses) are as follows: mini-G_s, 100 mg/L (65˚C); mini-G_{olf}, 80 mg/L (65˚C); mini-G_{o1} 100 mg/L (64˚C); mini-G_{12} 25 mg/L (73˚C). The worst expressed of the four new mini-G proteins was mini-G_{i1}, so an additional mutation G217D was incorporated and the truncation at the N-terminus shortened, which increased the yield of pure protein to 12 mg/L, although the stability was only 48˚C. Thus, mini-G_{olf}, mini G_{i1}, mini-G_{o1} and mini-G_{12} were all of sufficient stability to be used to test their ability to couple to relevant GPCRs. The amino acid sequences of the mini-G proteins are given in S1 Fig.

Four mini-G proteins were not expressed in *E. coli*, namely mini-G_z, mini-G_t, mini-G_{16} and mini-G_q (amino acid sequences are given in S2 Fig). The failure of the *en bloc* transfer of the deletions and mutations from mini-G_s, despite the high conservation of G protein structures, highlights our lack of understanding of the folding of these proteins. Indeed, it is well known that an accessory factor, Ric8, is required for the efficient folding of G_q in mammalian cells [33], and other unknown factors may also be required. For the purpose of this study, we therefore did not perform any further development of mini-G_{t1} and mini-G_z, given that two other members of the G_i family, mini-G_{i1} and mini-G_{o1}, already gave stable mini-G proteins. In contrast, as neither member of the G_q family tested produced a stable mini-G protein, we decided to develop alternative strategies to make a usable version of mini-G_q, whilst further work on mini-G_{16} was terminated. The successful engineering of a version of mini-G_q chimera will be discussed later.

Assay development and validation using the mini-G_s system

The ultimate goal of developing mini-G proteins is the structure determination of GPCRs in the fully active state bound to an agonist and a mini-G protein. In the simplest format, this necessitates the purification of the GPCR in detergents and forming the G protein–GPCR complex from the purified components *in vitro*. It was therefore essential to devise some simple assays that could assess whether a mini-G protein had coupled to a GPCR in detergent solution. This turned out to be not as straightforward as originally anticipated due to the potential instability of either the GPCR and/or mini-G protein in either their inactive and/or active conformations. These issues were not obvious when the original work on the development of mini-G_s was performed, because mini-G_s is one of the most stable mini-G proteins developed and also the thermostabilised β_1-adrenergic receptor (β_1AR) and the wild type adenosine A_{2A} receptor (A_{2A}R) were both much more stable than other GPCRs. We therefore developed five separate assays for assessing whether a mini-G protein coupled to a GPCR and/or formed a stable complex in detergent. These were all first tested using mini-G_s coupling to β_1AR and A_{2A}R. Each assay has its own limitations, which are often apparent in the subsequent sections where they were used on less stable receptors and the newly developed mini-G proteins, and these are discussed below. The five different assays that were used are the following:

(i) agonist affinity shift assay; (ii) thermostability assay (TSA); (iii) fluorescence-based saturation binding analysis (FSBA) of GFP-mini-G protein binding; (iv) fluorescence-detection size exclusion chromatography (FSEC); (v) size exclusion chromatography (SEC) of purified complex. A brief rationale for the use of each assay with their advantages and disadvantages are given below.

(i) Agonist affinity shift assay. The development of mini-G_s relied on the agonist affinity shift assay to identify those mutants that coupled to β_1AR [24]. It is generally considered that the defining feature of G protein coupling is an increase in the affinity of an agonist for the G protein–GPCR complex compared to the GPCR alone. For example, wild type β_2AR binds an agonist 100-fold more tightly when coupled to a G protein than the receptor alone [34]. However, the shift in agonist affinity in other receptors is often considerably smaller than that observed for β_2AR, such as the 10-fold shift in agonist affinity observed in β_1AR [34]. However, the advantage of this assay is that it can be performed using standard pharmacological procedures in high-throughput, using receptors in either membrane preparations or solubilized in detergent. Assays may use either a radiolabelled agonist in saturation binding experiments or, more usually, a radiolabelled antagonist in competition binding experiments [20, 24] (and see experiments below on the serotonin $5HT_{1B}$ receptor). The advantage of this assay is that it is very sensitive and can be performed on membrane-bound receptors *i.e.* in a format where the receptor is most stable in all conformations. The disadvantage of this assay is that it requires suitable radioligands for the receptor under study and these are not readily available for all GPCRs.

(ii) Thermostability assay. The thermostability of a detergent-solubilised GPCR depends upon the type of detergent used and whether the receptor is either ligand-free, agonist-bound or antagonist-bound [35, 36]. In addition, the receptor stability tends to be increased by an increase in affinity and/or decrease in the off-rate of the ligand [37]. Often, the agonist bound state is one of the least stable conformations of a receptor, presumably because agonists increase the probability of transitions to a fully active state. In the inactive state there is close packing of the intracellular surface of the transmembrane α-helices. Upon activation, the outward movement of helices 5 and 6 disrupts this close packed structure and creates a crevice where the C-terminus of the G protein binds, thus allowing G protein coupling [38]. The structures of non-rhodopsin GPCRs in the fully active state have been determined only when they have been stabilized through binding of a heterotrimeric G protein [2], a conformation-specific nanobody [15, 18, 19] or a mini-G protein [20]. The interface between a GPCR and a G protein is over 1000 $Å^2$ [2, 20], and is therefore predicted to increase the thermostability of the agonist-bound GPCR–G protein complex compared to the agonist-bound GPCR. This was observed for both β_1AR and A_{2A}R, which were consistently more stable in the agonist-bound state when coupled to mini-G_s in a variety of different detergents compared to when mini-G_s was absent [20, 24].

A typical thermostability assay measures how much of a radiolabelled agonist remains bound to a detergent-solubilised receptor after heating at different temperatures for 30 minutes [36]. The advantage of this assay is that it is fast and high-throughput and can be performed in any detergent of choice. Another advantage is that the agonist–GPCR–mini-G protein complex can be pre-formed in membranes, which may stabilise the receptor upon detergent solubilisation. If there is a shift in thermostability in the presence of a mini-G protein, then this is strongly suggestive of binding or coupling.

(iii) Fluorescence-detection size exclusion chromatography (FSEC). FSEC is a rapid methodology for assessing whether a membrane protein fused to GFP is stable in detergent by performing SEC on an unpurified detergent solubilisate and monitoring GFP fluorescence in the eluate [39]. A membrane protein stable in detergent gives a symmetrical peak at a size

consistent with the molecular weight of the membrane protein plus the mass of specifically bound detergent and lipid. By fusing GFP to the N-terminus of mini-G proteins (S3 Fig), it was possible to use FSEC to monitor whether a stable complex was formed between the mini-G protein and a GPCR. The GFP-mini-G_s fusion protein has a molecular weight of 54 kDa and migrated with a retention volume of 15.1 ml on FSEC. When this was mixed with either unpurified DDM-solubilised β_1AR or A_{2A}R in the presence of an agonist, then an additional peak was observed at 12.1–12.5 ml (Fig 3A and 3C), which was consistent with the molecular weight of the detergent-solubilised receptor bound to GFP-mini-G_s (~180 kDa). This additional peak was not observed if the receptors were bound to an inverse agonist. An additional peak was sometimes observed at a retention volume of 8 ml, which corresponds to the void volume of the SEC column and was due presumably to aggregates of GFP-mini-G_s.

The advantage of this assay is that it is a quick assessment of whether a GPCR forms a complex with a mini-G protein, because the receptor does not need to be purified and the SEC experiment takes under an hour. However, a major limitation is that only small amounts of GFP-mini-G_s can be used per experiment to avoid saturation of the detector and producing a very broad peak that would obscure the presence of the complex between the GPCR and GFP-mini-G protein. An additional limitation is the amount of membranes that can be solubilized efficiently using 0.5% DDM (to ensure maximal stability of mini-G_s; see below) and maintaining the small volume (500 μl) required for loading on the FSEC column (24 ml). Thus in the data shown (Fig 3A and Fig 3C) the amount of receptor is limiting and only a proportion of the GFP-mini-G_s is bound to receptor and is shifted in apparent molecular weight. In addition, the receptor–mini-G protein complex must be detergent-stable for a peak to be observed. Many GPCR–G protein complexes are too unstable to be observed in DDM and therefore it is essential to assess milder detergents such as LMNG (see section on the serotonin $5HT_{1B}$ receptor).

(iv) Fluorescence-based saturation binding analysis of mini-G protein binding. To determine the affinity of mini-G protein binding to a receptor, the fluorescence-based saturation binding assay (FSBA) was developed. In this assay, the amount of the GFP-mini-G protein specifically bound to an immobilized receptor was determined using a fluorescent plate reader. As proof of principle, DDM-solubilized β_1AR or A_{2A}R were immobilized onto Ni^{2+}-coated wells of a 96-well plate *via* their C-terminal poly-histidine tag, in the presence of either an agonist or inverse agonist. GFP-mini-G_s was then added at increasing concentrations. After washing to remove any non-specifically bound GFP-mini-G_s, the amount of GFP-mini-G_s fluorescence was measured (Fig 3B and 3D). GFP-mini-G_s showed a specific saturated binding to the receptor with apparent K_D values of 200 ± 1 nM (n = 2) and 430 ± 24 nM (n = 2) for GFP-mini-G_s binding to β_1AR and A_{2A}R, respectively.

The FSBA is a simple assay for determining the affinity of mini-G protein binding to a receptor *in vitro*. However, it must be appreciated that the apparent affinity determined may be specific only for the conditions in the assay. In particular, the type of detergent used may have a profound effect on the affinity, especially if it slightly destabilizes the active state of the receptor. The agonist may also affect the apparent affinity of the mini-G protein, depending on how effective the agonist is in stabilizing the active state of the receptor. However, the FSBA remains a useful tool for biophysical analyses of mini-G protein binding to a receptor.

(v) Size exclusion chromatography (SEC). The ultimate biochemical assay for observing coupling of mini-G proteins to a receptor is combining the purified components *in vitro* and then observing the co-elution of the relevant proteins on SEC [24]. Purified A_{2A}R and purified mini-G_s were mixed at a molar ratio of 1:1.2 in the presence of the agonist NECA, the complex allowed to form and then separation was performed by SEC. The A_{2A}R–mini-G_s complex resolved as a predominant peak with an apparent molecular weight of 153 kDa compared with

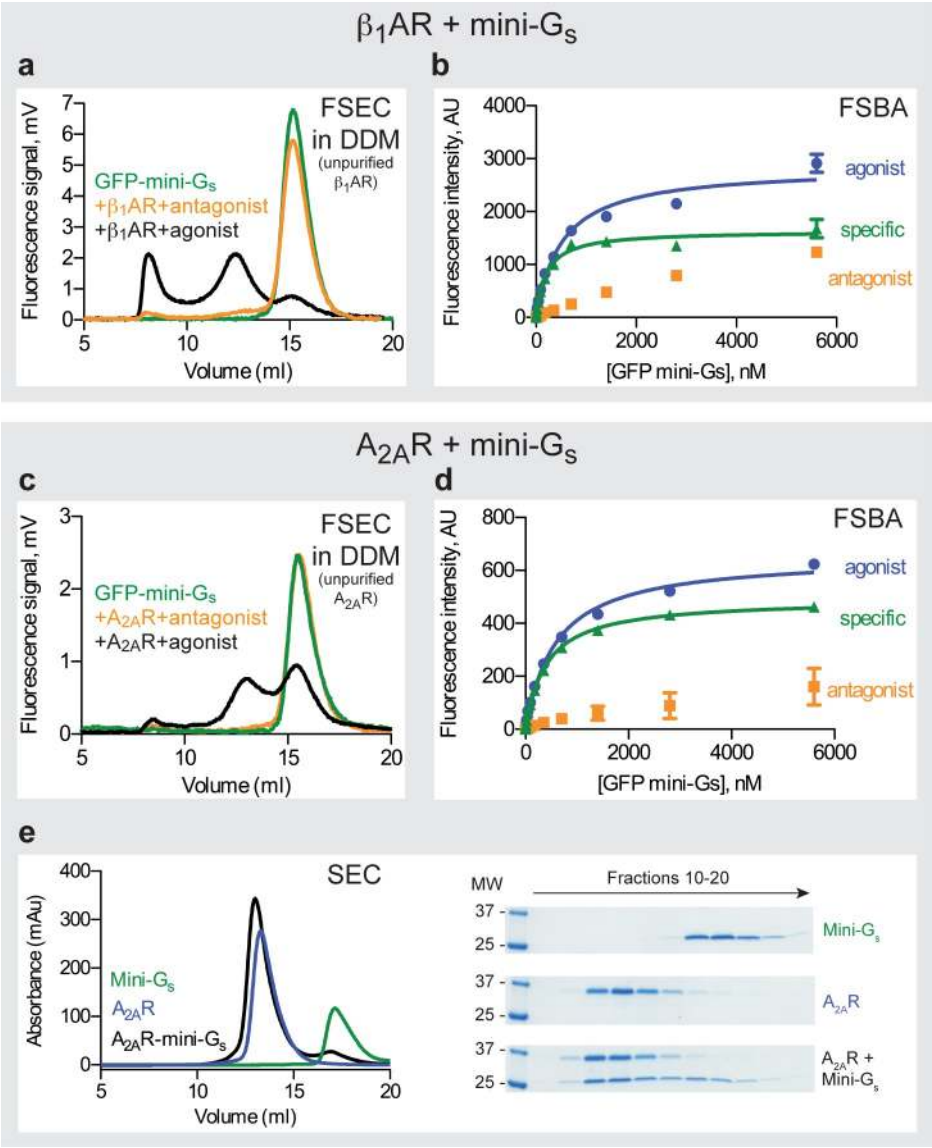

Fig 3. The β_1AR–mini-G_s and A_{2A}R–mini-G_s complexes. (**a**) FSEC traces of GFP-mini-G_s with β_1AR (retention volumes are given in parentheses): green, GFP-mini-G_s (15.1 ml); orange, GFP-mini-G_s with β_1AR bound to the inverse agonist ICI118551 (15.1 ml); black, GFP-mini-G_s with β_1AR bound to the agonist isoprenaline (8 ml, 12.1 ml and 15.1 ml). Representative chromatograms from at least two independent experiments are shown. (**b**) Measurement of GFP-mini-G_s affinity to DDM-solubilized β_1AR using a fluorescent saturation binding assay (FSBA); blue circles, β_1AR bound to the agonist isoprenaline (total binding); orange squares, β_1AR bound to the inverse agonist ICI118551 (non-specific binding); green triangles, specific binding, with an apparent K_D of 200 ± 1 nM (mean ± SEM, n = 2). Curves shown are from a representative experiment. (**c**) FSEC traces of GFP-mini-G_s with DDM-solubilised A_{2A}R (retention volumes are given in parentheses): green, GFP-mini-G_s (15.1 ml); orange, GFP-mini-G_s with A_{2A}R bound to the inverse agonist ZM241385 (15.1 ml); black, GFP-mini-G_s with A_{2A}R bound to the agonist NECA (12.5 ml and 15.1 ml). Representative chromatograms from at least two independent experiments are shown. (**d**) Measurement of mini-G_s affinity to DDM-solubilized A_{2A}R using FSBA: blue circles, A_{2A}R bound to the agonist NECA (total binding); orange squares, A_{2A}R bound to the inverse agonist ZM241385 (non-specific binding); green triangles, specific binding, with an apparent K_D of 430 ± 24 nM (mean ± SEM, n = 2). (**e**) Analytical size exclusion chromatography (SEC) of mini-G_s bound to purified A_{2A}R (retention volumes are given in parentheses): black, A_{2A}R–mini-G_s complex, 153 kDa (13 ml); blue, A_{2A}R, 133 kDa (13.3 ml); green, mini-G_s, 22 kDa (17.2 ml). Three panels to the right of the SEC traces are coomassie blue-stained SDS-PAGE gels of fractions from 3 separate SEC experiments: top panel, mini-G_s; middle panel, A_{2A}R; bottom panel, mini-G_s mixed with NECA-bound A_{2A}R (1.2:1 molar ratio).

https://doi.org/10.1371/journal.pone.0175642.g003

133 kDa for the receptor alone and 22 kDa for mini-G_s alone. SDS-PAGE analysis confirmed the presence of both $A_{2A}R$ and mini-G_s in fractions from the 153 kDa complex (Fig 3E).

The advantage of using purified components and SEC for analyzing complex formation is that complex formation is observed unambiguously. The conditions for complex formation can be refined and the stability of the complex can be assessed readily after a period of days by repeating the SEC. These data are essential for successful determination of the structure of a GPCR–mini-G protein complex. The disadvantage of this assay is that sufficient quantities of purified receptor are required and this may be limiting in the initial stages of a project. The limitation of the amount of purified receptor required for SEC may be partially overcome by analyzing complex formation using FSEC (see section on $5HT_{1B}R$).

Characterisation of mini-G proteins

Mini-G_{olf} couples and stabilizes $A_{2A}R$. The GTPase domains of G_{olf} and G_s share 87% sequence identity (80% for the full length α subunits) and both G proteins couple to $A_{2A}R$ [40]. Of the 17 amino acid residues in mini-G_s that make direct contact to residues in $A_{2A}R$ in the crystal structure of the $A_{2A}R$–mini-G_s complex [20], all of these residues are identical except that two Arg residues in G_s are replaced with two Lys residues in G_{olf}. Despite the high degree of sequence homology between these two isoforms, $G\alpha_{olf}$ is far more difficult to overexpress than $G\alpha_s$, in fact, the only method reported to produce functional $G\alpha_{olf}$ is co-expression with the molecular chaperone RIC8B in insect cells [41]. Therefore, we constructed mini-G_{olf} to investigate whether the mini-G protein version would be better expressed that native α subunit. Mini-G_{olf} was constructed by transferring the 7 point mutations and 3 deletions from mini-G_s (Fig 2) and mini-G_{olf} was highly expressed in *E. coli* and as stable as mini-G_s. The coupling of mini-G_{olf} to $A_{2A}R$ was assessed by SEC of the complex assembled *in vitro* from purified proteins and a thermostability assay [20, 24]. Purified NECA-bound $A_{2A}R$ was mixed with mini-G_{olf} and analysed by SEC and SDS-PAGE (Fig 4A). The apparent molecular weight of mini-G_{olf} was 23 kDa (17.1 ml; theoretical molecular weight 26 kDa) and the apparent molecular weight of purified $A_{2A}R$ in DM was 133 kDa (13.3 ml). The complex $A_{2A}R$–mini-G_{olf} resolved as a predominant peak with an apparent molecular weight of 153 kDa (13 ml) and

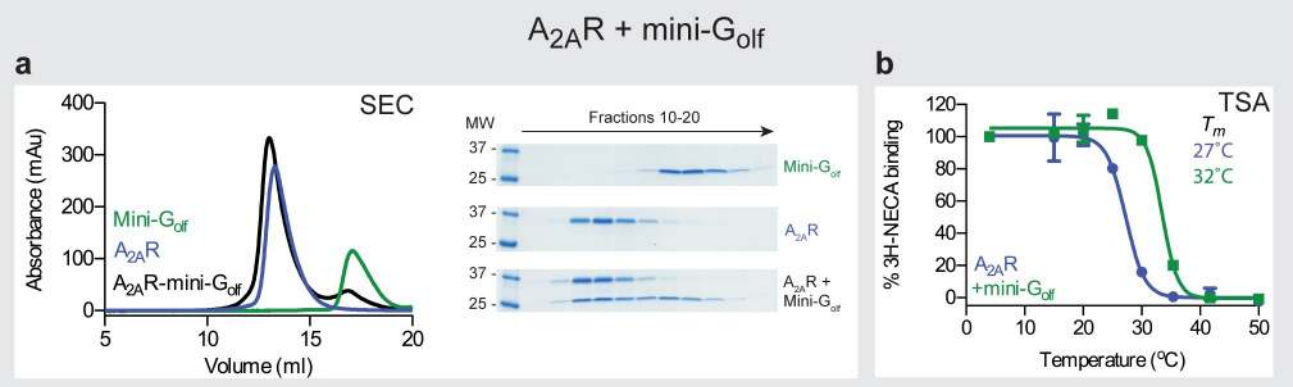

Fig 4. The $A_{2A}R$–mini-G_{olf} complex. (**a**) Analytical SEC of mini-G_{olf} bound to purified $A_{2A}R$ (retention volumes are given in parentheses): black, $A_{2A}R$–mini-G_{olf} complex, 153 kDa (13 ml); blue, $A_{2A}R$, 133 kDa (13.3 ml); green, mini-G_{olf}, 23 kDa (17.1 ml). Three panels to the right of the SEC traces are coomassie blue-stained SDS-PAGE gels of fractions from 3 separate SEC experiments: top panel, mini-G_{olf}; middle panel, $A_{2A}R$; bottom panel, mini-G_{olf} mixed with NECA-bound $A_{2A}R$ (1.2:1 molar ratio). (**b**) Thermostability assay (TSA) of unpurified DM-solubilized, ^{3}H-NECA-bound $A_{2A}R$. Data were analysed by nonlinear regression and apparent T_m values were determined from analysis of the sigmoidal dose-response curves fitted. T_m values represent mean±SEM of two independent experiments, each performed in duplicate: blue circles, no mini-G_{olf} (27 ± 0.3˚C); green squares, mini-G_{olf} (33 ± 1˚C). Curves shown are from a representative experiment.

https://doi.org/10.1371/journal.pone.0175642.g004

contained both $A_{2A}R$ and mini-G_{olf}. Mini-G_{olf} also stabilized agonist-bound DM-solubilised $A_{2A}R$, with mini-G_{olf}-coupled $A_{2A}R$ showing an apparent T_m of 32 ± 1˚C in comparison with 27 ± 0.3˚C for the receptor alone (Fig B). This stability was similar to that obtained with mini-G_s (33˚C) under the same conditions [20].

The results with mini-G_{olf} were very encouraging in terms of both the transferability of the mutations, the expression and stability of the mini-G_{olf} and the stability of the $A_{2A}R$–mini-G_{olf} complex. Thus where there is a high degree of homology between G proteins, then there is good transferability of the mutations, as was previously observed for the transfer of thermostabilising mutations between GPCRs [42]. These data also suggested that even if the native α subunit is poorly expressed the mini-G protein version may be highly expressed and very stable.

Development of chimeric mini-$G_{s/q}$ to study G_q-coupled receptors. The expression of mini-G_q in *E. coli* was unsuccessful. One possibility to explain this is that efficient folding of G_q *in vivo* is dependent on the molecular chaperone Ric8 [33] and that mini-G_q had a similar requirement. Indeed, co-expression of Ric8 with mini-G_q in the baculovirus expression system led to the overproduction of mini-G_q. However, upon purification of mini-G_q it was not possible to dissociate Ric8 (results not shown), suggesting that the mini-G_q was perhaps not correctly folded and/or was very unstable. Given the lack of success in transferring the mini-G protein mutations from G_s to G_q, another strategy was developed.

The second strategy used to try and develop mini-G_q was to transfer the specificity determinants of G_q onto mini-G_s. It is well established that the C-terminal region of a Gα subunit forms the main receptor binding site [43] and is one of the main determinants of coupling specificity [44, 45]. Mutating as few as 3–5 amino acids at the C-terminus of the G alpha subunit has been shown to switch the specificity of coupling to some GPCRs [44, 45]. However, the two GPCR–G protein structures published to date [2, 20] revealed an extensive interface between the receptors and Gα, suggesting that other regions of the G protein may also play a role in specificity. Recent *in vivo* FRET studies suggest that residues within the α5 helix, but distal to the five C-terminal residues, strongly influence specificity [46].

Mini-G_s did not couple to any of the G_q-coupled receptors tested (results not shown). We then evaluated a number of mini-$G_{s/q}$ chimeras (S4 Fig) for both gain of binding to G_q-coupled receptors (Fig 5A and 5B) and loss of binding to the cognate G_s-coupled receptor $A_{2A}R$, predominantly using thermostability assays (Fig 5C) and SEC (S5 Fig). First, the chimera mini-$G_{s/q}$57 was constructed in which the five C-terminal amino acids of mini-G_s ($Q^{H5.22}YELL^{H5.26}$) were changed to those found in $G\alpha_q$, which required three mutations ($Q390E^{H5.22}$, $E392N^{H5.24}$ and $L394V^{H5.26}$). There was no increase in thermostability of agonist-bound AT_1R or NTSR1 in the presence of mini-$G_{s/q}$57 that might suggest coupling (Fig 5A and 5B). In fact, there was a decrease in thermostability of AT_1R in the presence of mini-$G_{s/q}$57, suggesting that binding had occurred, but that residues of G_s were clashing with the receptor and causing its destabilisation. Furthermore, a complex between mini-$G_{s/q}$57 and $A_{2A}R$ was still observed (Fig 5C and S5 Fig), suggesting that the mutations were insufficient to change the specificity of G_s to G_q. Therefore, the chimera mini-$G_{s/q}$58 was constructed in which the final 19 amino acid residues in the α5 helix of mini-G_s ($Phe376^{H5.8}$—$Leu394^{H5.26}$) were changed to those in $G\alpha_q$; this required 13 mutations ($N377A^{H5.9}$, $D378A^{H5.10}$, $C379V^{H5.11}$, $R380K^{H5.12}$, $I382T^{H5.14}$, $Q384L^{H5.16}$, $R385Q^{H5.17}$, $M386L^{H5.18}$, $H387N^{H5.19}$, $R389K^{H5.21}$, $Q390E^{H5.22}$, $E392N^{H5.24}$ and $L394V^{H5.26}$). Mini-$G_{s/q}$58 did not couple to $A_{2A}R$ (Fig 5C and S5 Fig), demonstrating that residues in the α5 helix beyond the C-terminal 5 amino acids are important in G protein specificity. However, there was no significant shift in the thermostability of the G_q-coupled receptor NTSR1 in the presence of mini-$G_{s/q}$58 (Fig 5B). We reasoned that this may be because the stability of mini-$G_{s/q}$58 was impaired, because mutating the last 19 amino acid residues in mini-G_s would have also changed residues buried in

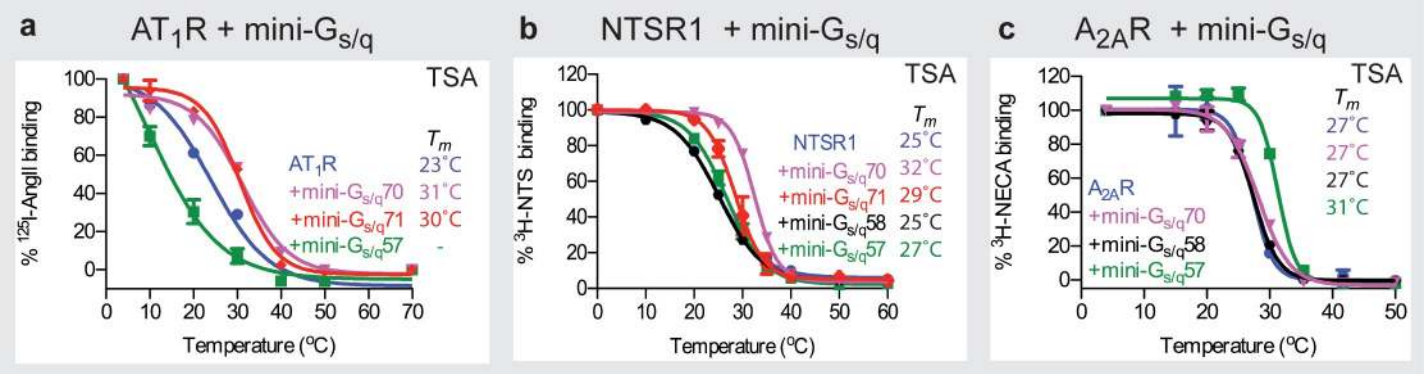

Fig 5. Thermostability assays of various complexes between mini-$G_{s/q}$ chimeras and GPCRs. (**a**) Thermostability of unpurified digitonin-solubilized, ^{125}I-AngII-bound AT_1R (T_m values in parentheses): blue circles, no mini-$G_{s/q}$ (23 ± 0.4˚C); green squares, mini-$G_{s/q}$57 (T_m not determined); magenta inverted triangles, mini-$G_{s/q}$70 (31 ± 1˚C); red triangles, mini-$G_{s/q}$71 (30 ± 0.8˚C). (**b**) Thermostability of unpurified DDM-solubilized, ^{3}H-NTS-bound NTSR1: blue, no mini-$G_{s/q}$ (25 ± 0.4˚C); green squares, mini-$G_{s/q}$57 (27 ± 0.7˚C); black circles, mini-$G_{s/q}$58 (25 ± 0.4˚C); magenta inverted triangles, mini-$G_{s/q}$70 (32 ± 0.3˚C); red diamonds, mini-$G_{s/q}$71 (29 ± 1.1˚C). (**c**) Thermostability of unpurified DM-solubilized, ^{3}H-NECA-bound $A_{2A}R$: blue circles, no mini-$G_{s/q}$ (27 ± 0.3˚C); green squares, mini-$G_{s/q}$57 (31 ± 0.3˚C); black circles, mini-$G_{s/q}$58 (27 ± 0.5˚C); magenta inverted triangles, mini-$G_{s/q}$70 (27 ± 0.2˚C). In all panels, data (n = 3) were analysed by nonlinear regression and apparent T_m values were determined from analysis of the sigmoidal dose-response curves fitted with values shown as mean ± SEM. Curves shown are from a representative experiment.

https://doi.org/10.1371/journal.pone.0175642.g005

the core of the G protein, thus affecting the stability of the mini-G_s backbone. Therefore, a refined version of this chimera, mini-$G_{s/q}$70, was constructed in which residues in the α5 helix whose side chains formed direct contacts (3.9 Å cut-off) with either β_2AR [2] or $A_{2A}R$ [20] in the G protein-bound structures were mutated to match those in $G\alpha_q$ (R380K$^{H5.12}$, Q384L$^{H5.16}$, R385Q$^{H5.17}$, H387N$^{H5.19}$, E392N$^{H5.24}$ and L394V$^{H5.26}$; S4 Fig). In addition, the mutation Q390E$^{H5.22}$ was included, despite only making contact to $A_{2A}R$ via its backbone, as it is buried in the receptor–G protein interface and may be important for binding to G_q-coupled receptors. Mini-$G_{s/q}$70 gave better binding to both G_q-coupled receptors tested, NTSR1 and AT_1R, and showed no binding to $A_{2A}R$ (Fig 5 and S5 Fig).

Two other chimeras were also constructed to try and improve on mini-$G_{s/q}$70. Mini-$G_{s/q}$72 contained the additional mutation C379V$^{H5.11}$ compared to mini-$G_{s/q}$70 and, although the C379$^{H5.11}$ side chain does not form direct contacts with either $A_{2A}R$ or β_2AR, its mutation to Val is predicted to introduce a direct interaction between the Val γ2 carbon and Leu110 from $A_{2A}R$. However, the AT_1R–mini-$G_{s/q}$72 complex did not have a higher thermostability than AT_1R–mini-$G_{s/q}$70 (results not shown). Finally, the chimera mini-$G_{s/q}$71 was constructed in which residues from other regions of Gα that form direct contacts with either β_2AR [2] or $A_{2A}R$ [20] were mutated to match those in $G\alpha_q$. This included the seven mutations in mini-$G_{s/q}$70 (R380K$^{H5.12}$, Q384L$^{H5.16}$, R385Q$^{H5.17}$, H387N$^{H5.19}$, Q390E$^{H5.22}$, E392N$^{H5.24}$ and L394V$^{H5.26}$) and six additional mutations (A39R$^{HNS1.3}$, H41L$^{S1.2}$, D343K$^{H4.23}$, L346V$^{H4.26}$, R347D$^{H4.27}$ and Y358I $^{H4S6.11}$). D343$^{H4.23}$ was the only amino acid residue whose side chain did not interact with either $A_{2A}R$ or β_2AR, but the mutation to Lys was included because the longer side chain could potentially interact with a receptor and the charge reversal may be important for specificity. Conversely, Thr350$^{H4S6.3}$ was *not* mutated to Pro in mini-$G_{s/q}$71 even though its side chain forms direct contacts with β_2AR. Alignment of $G\alpha_s$ with two independently solved structures of $G\alpha_q$ [47, 48] showed that this region of the G proteins differ significantly and thus, in $G\alpha_q$, this residue is unlikely to interact with the receptor. However, after all these considerations to make an improved version of mini-$G_{s/q}$70, mini-$G_{s/q}$71 did not improve the thermostability of agonist-bound G_q-coupled receptors compared to mini-$G_{s/q}$70 (Fig 5A and 5B).

Mini-G_{i1}: Tackling stability issues. Transfer of the 7 point mutations and 3 deletions from mini-G_s into $G\alpha_{i1}$ to make mini-G_{i1} was not successful, as the resultant protein was very

poorly expressed and had low stability (results not shown). Whilst the work on developing chimeras of mini-$G_{s/q}$ was underway, we decided to first study the reasons why mini-G_{i1} appeared to be so unstable. Therefore, to improve expression, stability and to allow binding of the mini-G_{i1} to the βγ subunits, the N-terminus (residues 4–18) was re-inserted, $Asp249^{H3.8}$ was mutated back to Leu, and the $G217D^{H2S4.3}$ mutation introduced based on a sequence comparison between G_{i1} (poorly expressed) and G_s/G_o (highly expressed) (Fig 2 and S1 Fig). The resultant mini-G_{i1} (construct 46) yielded only 12 mg of purified protein per litre of culture and was 17˚C less stable than mini-G_s, but was suitable for initial studies in GPCR coupling.

The serotonin $5HT_{1B}$ receptor ($5HT_{1B}R$) was used as a model G_i-coupled receptor for developing mini-G_{i1} because it could be expressed and purified in DDM using the baculovirus expression system and its structure determined in the inactive state. Initially, GFP-mini-G_{i1} was tested using FSEC for binding to purified $5HT_{1B}R$ (in DDM) and bound to the agonist donitriptan. However, the GFP-mini-G_{i1} (S3 Fig) migrated at 13.5 ml in the absence of receptor or in the presence of donitriptan-bound $5HT_{1B}R$, indicating that no coupling occurred (Fig 6C). However, when the LMNG-purified $5HT_{1B}R$ was used, the FSEC showed two peaks, one corresponding to free GFP-mini-G_{i1} with a retention volume of 14.3 ml and the other corresponding to GFP-mini-G_{i1} bound to donitriptan-activated $5HT_{1B}R$, with a retention volume of 12.2 ml (Fig 6D). The presence of two peaks, suggested that mini-G_{i1} was not stable in detergent when in a complex with $5HT_{1B}R$. The detergent instability of the complex could also have been due to the receptor, but because agonist-bound $5HT_{1B}R$ had been crystallised previously [10], we felt this was unlikely. In order to improve the stability of mini-G_{i1}, the heterotrimer was formed between GFP-mini-G_{i1}46 (S3 Fig) and $\beta_1\gamma_2$ and tested by FSEC. The GFP-mini-trimer in complex with the LMNG-purified $5HT_{1B}R$ resolved as a single peak with a retention volume of 11.8 ml compared to 14.3 ml for the free GFP-mini-$G_{i1}\beta_1\gamma_2$ trimer (Fig 6F). Thus the $\beta_1\gamma_2$ subunits restored the stability of mini-G_{i1}.

Although the mini-$G_{i1}\beta_1\gamma_2$ trimer coupled successfully to LMNG-solubilised $5HT_{1B}R$, this is not as desirable for crystallography as a mini-G protein coupled receptor due to the large size of the heterotrimeric G protein. Therefore, following the successful strategy of changing the coupling of mini-G_s to that of G_q by making a mini-$G_{s/q}$ chimera, the same strategy was applied to engineer a mini-$G_{s/i1}$ chimera (S1 Fig and S6 Fig). Therefore 9 mutations ($C379V^{H5.11}$, $R380T^{H5.12}$, $Q384I^{H5.16}$, $R385K^{H5.17}$, $H387N^{H5.19}$, $Q390D^{H5.22}$, $Y391C^{H5.23}$, $E392G^{H5.24}$ and $L394F^{H5.26}$) were introduced into the α5 helix of mini-G_s to change its coupling specificity to that of G_{i1}. A complex between GFP-mini-$G_{s/i1}$43 (S3 Fig) with donitriptan-bound DDM-purified $5HT_{1B}R$ resolved as a single peak with a retention volume of 13.2 ml compared to 15.1 ml for the free GFP-mini-$G_{s/i1}$ (Fig 6E). Thus mini-$G_{s/i1}$ was indeed more stable than mini-G_{i1}. The specificity of mini-G_s compared to mini-$G_{s/i1}$ for donitriptan-bound, DDM-solubilised $5HT_{1B}R$ was confirmed using FSBA (Fig 6B). No specific coupling of GFP-mini-G_s to $5HT_{1B}R$ was observed, although specific coupling to GFP-mini-$G_{s/i1}$ (apparent K_D 390 nM; Fig 6B) was confirmed.

In order to compare all of the mini-G_{i1} constructs and the role of $\beta_1\gamma_2$, agonist affinity shift assays were performed on $5HT_{1B}R$. The uncoupled receptor showed a K_i for the agonist sumatriptan in this assay of 280 ± 10 nM, which was shifted by mini-G_{i1}46 and mini-$G_{s/i1}$43 to 80 ± 13 nM and 36 ± 2 nM, respectively (Fig 6A). However, addition of $\beta_1\gamma_2$ to the mini-G proteins resulted in a further increase in agonist affinity to 15 ± 1 nM and 7.2 ± 0.8 nM for mini-G_{i1}46-$\beta_1\gamma_2$ and mini-$G_{s/i1}$43-$\beta_1\gamma_2$, respectively. Thus despite the successful generation of both mini-G_{i1} and mini-$G_{s/i1}$, their stability is still not perfect as binding of $\beta_1\gamma_2$ stabilises the mini-G proteins and elicits a greater increase in agonist affinity upon coupling of the mini-trimers.

Coupling of mini-G_{o1} to $5HT_{1B}R$. The GTPase domain of G_{o1} and G_{i1} are highly conserved (80% identity), but the mini-G proteins derived from them behaved very differently.

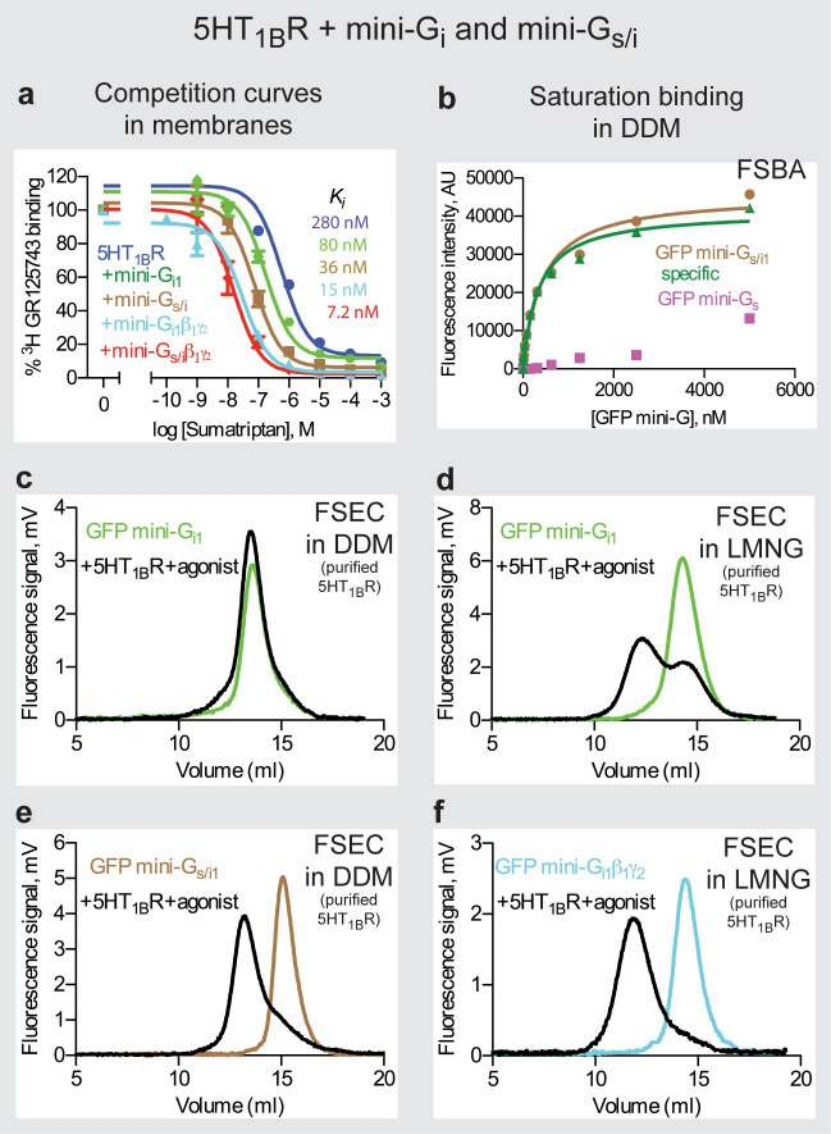

Fig 6. The $5HT_{1B}R$–mini-G_{i1} complexes. (**a**) Mini-G_{i1} coupling increases agonist affinity to $5HT_{1B}R$. Competition binding curves were performed in duplicate (n = 2) by measuring the displacement of the antagonist ^{3}H-GR125743 with increasing concentration of the agonist sumatriptan (K_i values representing mean ± SEM in parentheses): blue circles, $5HT_{1B}R$ (K_i 280 ± 10 nM); green hexagons, $5HT_{1B}R$ and mini-G_{i1} (K_i 80 ± 13 nM); brown squares, $5HT_{1B}R$ and mini-$G_{s/i1}$ (K_i 36 ± 2 nM); pale blue triangles, $5HT_{1B}R$ and mini-$G_{i1}\beta_1\gamma_2$ (K_i 15 ± 1 nM); red diamonds, $5HT_{1B}R$ and mini-$G_{s/i1}\beta_1\gamma_2$ (K_i 7.2 ± 0.8 nM). Error bars represent the SEM. (**b**) Measurement of mini-$G_{s/i1}$ chimera affinity to the DDM-solubilized, donitriptan-bound $5HT_{1B}R$ using FSBA: brown circles, $5HT_{1B}R$ and GFP-mini-$G_{s/i1}$ (total binding); purple squares, $5HT_{1B}R$ and GFP-mini-G_s (non-specific binding); green triangles, specific binding. The apparent K_D of 390 ± 47 nM represents the mean ± SEM of two independent experiments. Curves shown are from a representative experiment. (**c**) FSEC traces of GFP-mini-G_{i1} with $5HT_{1B}R$ in DDM: black, GFP-mini-G_{i1} and donitriptan-bound $5HT_{1B}R$ purified in DDM (13.5 ml); green GFP-mini-G_{i1} (13.5 ml). (**d**) FSEC traces of GFP-mini-G_{i1} with $5HT_{1B}R$ in LMNG: black, GFP-mini-G_{i1} and donitriptan-bound $5HT_{1B}R$ purified in LMNG (12.2 ml and 14.3 ml); green, GFP-mini-G_{i1} (14.3 ml). (**e**) FSEC traces of GFP-mini-$G_{s/i1}$ with $5HT_{1B}R$: black, GFP-mini-$G_{s/i1}$ and donitriptan-bound $5HT_{1B}R$ purified in DDM (13.2 ml); brown, GFP-mini-$G_{s/i1}$ (15.1 ml). (**f**) FSEC traces of GFP-mini-$G_{i1}\beta_1\gamma_2$ with $5HT_{1B}R$: black, GFP-mini-$G_{i1}\beta_1\gamma_2$ and donitriptan-bound $5HT_{1B}R$ purified in LMNG (11.8 ml); pale blue, GFP-mini-$G_{i1}\beta_1\gamma_2$ (14.3 ml). In panels **c-f**, retention volumes are given in parentheses.

https://doi.org/10.1371/journal.pone.0175642.g006

Unlike the unstable mini-G_{i1}, mini-G_{o1} expressed well (100 mg/L), had high stability comparable to mini-G_s and it was largely insensitive to the presence of mild detergents. Since $5HT_{1B}R$ couples to both G_o and G_i family members [49], we tested mini-G_{o1} coupling to $5HT_{1B}R$ and compared the results to coupling with mini-G_{i1} (see above). On FSEC, GFP-mini-G_{o1}12 (S3 Fig) partially coupled to donitriptan-bound, DDM-solubilised $5HT_{1B}R$ (unpurified), with the higher molecular weight species (retention volume 13 ml) reduced when the receptor was bound to an antagonist (Fig 7C). This was in contrast to the results with mini-G_{i1} under the same conditions where no binding was observed (Fig 6C). The partial coupling probably resulted from the low amount of $5HT_{1B}R$ used in the assay, because when the experiment was repeated using purified $5HT_{1B}R$ and GFP-mini-G_{o1}, all of the GFP-mini-G_{o1} bound to the receptor (Fig 7E). This is consistent with what was observed for β_1AR and $A_{2A}R$ (Fig 3). The $5HT_{1B}R$–mini-G_{o1} complex was purified by SEC and SDS-PAGE indicated co-elution of $5HT_{1B}R$ and mini-G_{o1} in a 1:1 molar ratio (Fig 7D). GFP-mini-G_{o1} bound to DDM-solubilised $5HT_{1B}R$ in the presence of donitriptan with an apparent K_D of 180 ± 24 nM (Fig 7B). In membranes, mini-G_{o1}12 shifted the agonist affinity for $5HT_{1B}R$ from 280 ± 10 nM to 32 ± 3 nM (Fig 7A).

The properties of mini-G_{o1} make this an ideal choice for structural studies of G_o/G_i coupled receptors, rather than using mini-$G_{s/i}$, as it is more highly expressed and more tolerant of detergents. This is exemplified by the stability of the donitriptan-bound $5HT_{1B}R$–mini-G_{o1} complex made from purified components (S7 Fig).

Conclusions

The aim of the work presented here was to generate a range of mini-G proteins that could be used as a basis for the structure determination of GPCRs in their fully active state. The original work in developing mini-G proteins was performed on G_s [24], which turned out to be one of the best expressed and most stable of the mini-G proteins. The structures of GPCRs and G proteins are highly conserved [4], and there are thought to be highly conserved networks of side chain interactions within the GPCR [5] and G protein [6] that are essential for receptor activation and G protein activation. It therefore seemed reasonable to use the two G_s-coupled GPCR structures [2, 20] to guide the engineering of G_i, G_o or G_q, given that there are no structures of receptors coupled to these G proteins. Transfer of the relevant mutations from mini-G_s to other G proteins was successful in deriving mini-G_{olf}, mini-G_{o1} and mini-G_{12}. Both mini-G_{olf} and mini-G_{o1} coupled to relevant receptors only in the presence of an agonist and formed stable complexes that could be purified by SEC. Currently, we have not been able to demonstrate binding of mini-G_{12} to any receptor (results not shown), even though it is highly expressed in *E. coli* and has high thermal stability, suggesting that the protein is in a folded state. In contrast, initial trials to generate mini-G_{t1}, mini-G_z mini-G_q and mini-G_{16} were unsuccessful due to no expression in *E. coli*; we have not yet tested the chimera strategy on these targets. Mini-G_{i1} expressed very poorly, but was improved upon further mutagenesis, but was still not as stable as mini-G_s and required binding of βγ subunits to attain a full agonist affinity shift in the $5HT_{1B}R$.

The second approach to generate mini-G proteins for those that did not work initially was to make chimeras by converting the specificity of mini-G_s to the specificity of the desired G protein. This was developed initially for G_q by mutating in mini-G_s only those residues in the α5 helix whose side chains make contact to either β_2AR or $A_{2A}R$ in the crystal structures of the relevant complexes [2, 20], to match the equivalent residues in G_q. The final mini-$G_{s/q}$ chimera was stable, overexpressed in *E. coli* and coupled to G_q-coupled receptors, but not to G_s-coupled receptors. The process was also successful in generating a mini-$G_{s/i1}$ and mini-$G_{s/o}$ chimera.

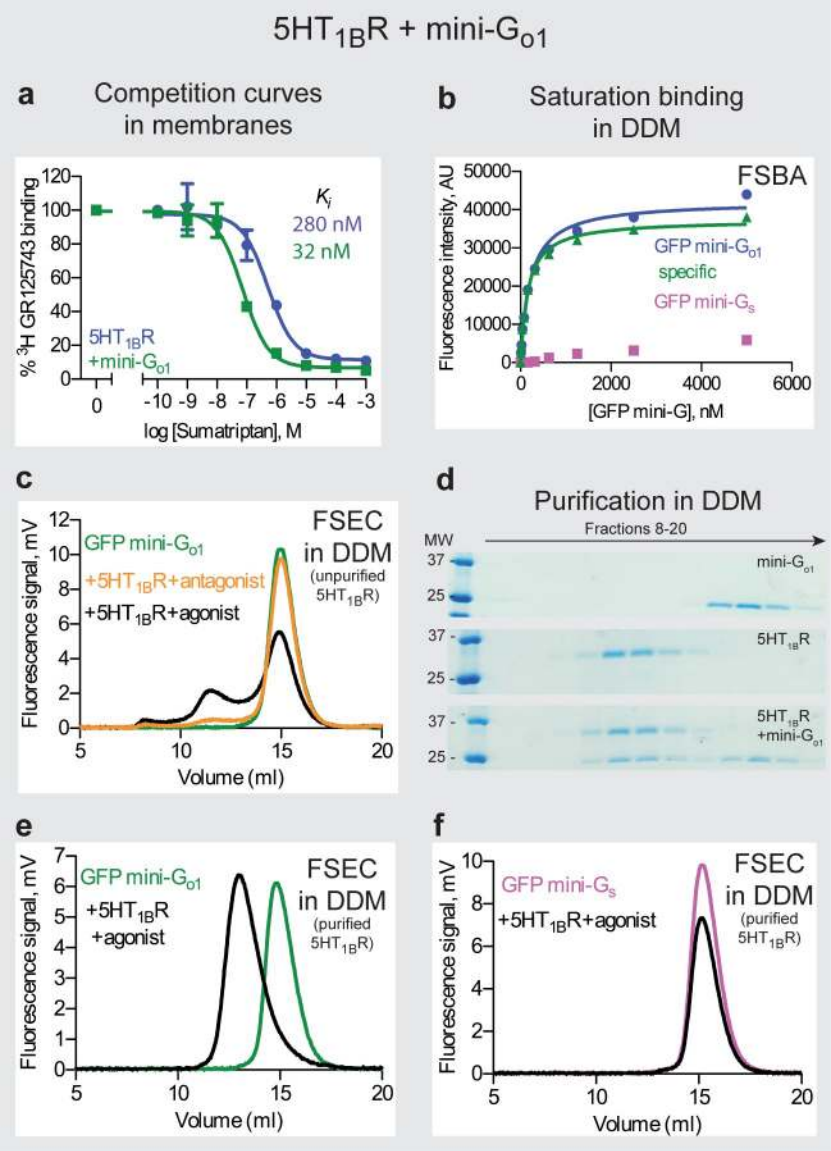

Fig 7. The $5HT_{1B}R$–mini-G_{o1} complex. (**a**) Competition binding curves were performed on membranes in duplicate (n = 2) by measuring the displacement of the antagonist ^{3}H-GR125743 with increasing concentration of the agonist sumatriptan (apparent K_i values representing mean ± SEM are in parentheses): blue circles, $5HT_{1B}R$ (K_i 280 ± 10 nM); green squares, $5HT_{1B}R$ and mini-G_{o1} (K_i 32 ± 3 nM). Error bars represent SEM. (**b**) Measurement of GFP-mini-G_{o1} affinity to DDM-solubilized, donitriptan-bound $5HT_{1B}R$ using the FSBA: blue circles, $5HT_{1B}R$ and GFP-mini-G_{o1} (total binding); purple squares, $5HT_{1B}R$ and GFP-mini-G_s (non-specific binding); green triangles, specific binding. The apparent K_D value (180 ± 24 nM) represents mean ± SEM of two independent experiments. Curves shown are from a representative experiment. (**c**) FSEC traces of GFP-mini-G_{o1} with DDM-solubilized unpurified $5HT_{1B}R$ bound to the following (retention volumes are shown in parentheses): orange, the antagonist SB224289 (14.9 ml); black, the agonist donitriptan (11.3 ml and 14.9 ml). Free GFP-mini-G_{o1} (green) resolved as a predominant peak with a retention volume of 14.9 ml (**d**) Mini-G_{o1} forms a complex with purified $5HT_{1B}R$. The three panels are coomassie blue-stained SDS-PAGE gels of fractions from 3 separate SEC experiments: top panel, mini-G_{o1}; middle panel, $5HT_{1B}R$; bottom panel, mini-G_{o1} mixed with donitriptan-bound $5HT_{1B}R$ (1:1 molar ratio). (**e**) FSEC traces of GFP-mini-G_{o1} with purified $5HT_{1B}R$: black, GFP-mini-G_{o1} with $5HT_{1B}R$ purified in DDM (13 ml); green, GFP-mini-G_{o1} (14.8 ml). (**f**) FSEC traces of GFP-mini-G_s with purified $5HT_{1B}R$: black, GFP-mini-G_s with $5HT_{1B}R$ purified in DDM (negative control; 15.1 ml); purple, GFP-mini-G_s (15.1 ml). Retention volumes are shown in parentheses.

https://doi.org/10.1371/journal.pone.0175642.g007

Table 1. Mini-G proteins and their characteristics.

Mini-G protein	Construct	Yield of pure protein per L of *E. coli* (mg)	Stability measured by DSF (˚C)	Stability in detergent measured by native DSF (˚C)		
				No detergent	0.1% LMNG	0.1% DDM
G_s	393	100	65 ± 0.0	48 ± 0.2	45 ± 0.2	39 ±0.0
G_{olf}	6	80	65 ± 0.4	44 ± 0.1	42 ± 0.0	37 ± 0.2
$G_{s/q}$	70	50	67 ± 0.4	47 ± 0.3	44 ± 0.2	36 ±0.1
$G_{s/i1}$	43	40	69 ± 0.1	45 ± 0.0	41 ± 0.1	36 ± 0.1
G_{o1}	12	100	64 ± 0.1	44 ± 0.2	41 ± 0.1	33 ±0.2
G_{12}	8	25	73 ± 0.3	50 ± 0.1	46 ± 0.1	41 ± 0.2

https://doi.org/10.1371/journal.pone.0175642.t001

The α5 helix provides ~70% of the buried surface area between the GTPase domain and the receptor in the two G protein–GPCR complexes crystallised to date. The work here shows that changing these contacts is sufficient to alter the specificity of coupling. However, this is not to say that the remaining 30% of the interface is not important, merely that a range of amino acid residues can be accommodated in this interface and therefore it plays a less important role in defining both specificity and the affinity of G protein binding.

The mini-G proteins and their properties are shown in Table 1 and Table 2. On the whole, the expression levels are satisfactory in *E. coli* and the stability of the mini-G proteins in the absence of detergent is also good. However, their stability decreases in detergent, particularly in high concentrations, with the greatest decrease in stability observed at high detergent concentrations (greater than 0.5% w/v) and with detergents that are regarded as harsh for membrane protein purification [50]. Thus care must be exercised in the initial choice of detergent for forming receptor–mini-G protein complexes. However, GPCRs in the active state are also unstable in detergent and this also needs to be carefully addressed before structural studies are a possibility. This may require the use of very high-affinity agonists that stabilize the receptor and/or the stabilisation of the GPCR–mini-G protein complex by conformational thermostabilisation. It is not trivial to define which component, receptor or mini-G protein, is the least stable within a complex under a given set of conditions. This is why we recommend that initial tests are performed on the receptor solubilized in very mild detergents such as digitonin, GDN or LMNG.

Despite the successes described here, mini-G proteins are not a panacea for all GPCRs. The specificity determinants for G protein coupling are not determined solely by the α5 helix and the subtypes of βγ can also affect the efficiency and specificity of coupling within a cell [51, 52]. As we have not taken any subtype-specific G protein-GPCR interactions into account, further engineering of the mini-G proteins in the light of new structural data of GPCRs coupled to G_i, G_o or G_q may improve their performance further. Additional complications to making stable receptor–G protein complexes are the kinetics of dissociation of the G protein from the

Table 2. Mini-G proteins that bind βγ subunits and their characteristics.

Mini-G protein that bind βγ	Construct	Yield of pure protein per L of *E. coli* (mg)	Stability measured by DSF (˚C)
G_s	399	100	72 ± 0.0
G_{olf}	9	144	66 ± 0.1
$G_{s/q}$	76	30	71 ± 0.1
G_{i1}	46	12	48 ± 0.3
$G_{s/i1}$	48	10	72 ± 0.1
$G_{s/o1}$	16	15	69 ± 0.1

https://doi.org/10.1371/journal.pone.0175642.t002

activated receptor and the stability of the activated receptor itself. There has probably been strong evolutionary pressure for some GPCRs to evolve transient signaling complexes that are inherently unstable to provide tight regulation of the signaling process. Thus it may be necessary to thermostabilise the receptor in the active conformation [36] to generate a complex sufficiently stable for structural studies, although for other GPCR–G protein complexes this may not be necessary.

Supporting information

S1 Fig. Sequence of mini-G proteins used in this study. The poly-histidine tag is highlighted in red, the TEV protease cleavage site is highlighted in grey, and the linker used to replace the GαAH domain is highlighted in turquoise. Mutations are shown in bold type and underlined.
(DOCX)

S2 Fig. Sequence of mini-G proteins that were *not* successfully expressed in *E. coli*. The poly-histidine tag is highlighted in red, the TEV cleavage site highlighted in grey and the linker used to replace the GαAH domain is highlighted in turquoise. Mutations are shown in bold type and underlined. The constructs were cloned into plasmid pET15b for *E. coli* expression using *Nco*I (yellow) and *Xho*I (magenta) restriction sites. Start and stop codons are in red.
(DOCX)

S3 Fig. Sequence of GFP-mini-G proteins used in this study. GFP (highlighted in green) was fused to the N-terminus of the mini-G proteins with a GGGGS linker (highlighted in yellow). The poly-histidine tag is highlighted in red, the TEV cleavage site highlighted in grey and the linker used to replace the GαAH domain is highlighted in turquoise.
(DOCX)

S4 Fig. Sequence alignment of selected mini-$G_{s/q}$ chimeras used in this study. Residues in red are the signature mutations of a mini-G protein. Residues in blue are those found in G_q. Diamonds above the sequences identify the amino acid residues in $G\alpha_s$ where the side chains that make atomic contacts to residues in either β_2AR (β2 con) or A_{2A}R (2A con). Ovals above the sequences identify the amino acid residues in $G\alpha_s$ where only the main chain atoms make contacts to the receptor.
(DOCX)

S5 Fig. Analytical SEC and SDS-PAGE analyses of purified A_{2A}R with mini-$G_{s/q}$ chimeras. Analytical SEC of mini-$G_{s/q}$57 (**a**), mini-$G_{s/q}$58 (**b**) and mini-$G_{s/q}$70 (**c**) bound to purified A_{2A}R: black, A_{2A}R–mini-$G_{s/q}$ complex; blue, A_{2A}R; green, mini-$G_{s/q}$. Three panels below the SEC traces are coomassie blue-stained SDS-PAGE gels of fractions from 3 separate SEC experiments: top panel, mini-$G_{s/q}$; middle panel, A_{2A}R; bottom panel, NECA-bound A_{2A}R mixed with mini-$G_{s/q}$ (1:1.2 molar ratio).
(PDF)

S6 Fig. Sequence alignment of the different mini-G_{i1} and mini-G_{o1} proteins used in this study. Residues in red are the signature mutations of a mini-G protein. Note the additional G217D mutation (highlighted in yellow; residue 114 in the mini-G protein) in mini-G_{i1} to improve expression. Residues highlighted in cyan in mini-G_s were mutated to their equivalent in mini-G_{i1} or mini-G_{o1} (highlighted in magenta and grey respectively) to make the mini-$G_{s/i1}$ or mini-$G_{s/o1}$ chimeras. Note the re-insertion of the N-terminus and the back mutation (D to L) highlighted in green in the constructs that were used to form a heterotrimer with $\beta_1\gamma_2$ (*i.e.* mini-G_{i1}_46; mini-$G_{s/i1}$_43 and mini-$G_{s/o1}$_16).
(PDF)

S7 Fig. Stability of the purified donitriptan-bound $5HT_{1B}R$–mini-G_{o1} complex. (a) The complex was assembled from purified components and analysed by SEC immediately after assembly (blue line) or after the sample was stored at 4˚C for 48h (red line). Fractions (0.5 ml) were collected and analysed by SDS-PAGE: (b) immediately after assembly; (c) after 48 h at 4˚C.
(PDF)

Acknowledgments

We thank F. Marshall for helpful comments in the preparation of the manuscript.

Author Contributions

Conceptualization: RN BC CGT.

Formal analysis: RN BC Singhal A. Strege CFW HD.

Funding acquisition: CGT RG.

Investigation: RN BC A. Singhal A. Strege CFW HD.

Methodology: RN BC.

Project administration: CGT RG.

Resources: PE BC RN.

Supervision: RG CGT.

Validation: RN BC A. Singhal A. Strege CFW HD RG CGT.

Visualization: RN CGT.

Writing – original draft: RN CGT.

Writing – review & editing: RN BC A. Singhal RG CGT.

References

1. Rosenbaum DM, Rasmussen SG, Kobilka BK. The structure and function of G-protein-coupled receptors. Nature. 2009; 459(7245):356–63. PubMed Central PMCID: PMCPMC3967846. https://doi.org/10.1038/nature08144 PMID: 19458711
2. Rasmussen SG, DeVree BT, Zou Y, Kruse AC, Chung KY, Kobilka TS, et al. Crystal structure of the beta2 adrenergic receptor-Gs protein complex. Nature. 2011; 477(7366):549–55. Epub 2011/07/21. PubMed Central PMCID: PMC3184188. https://doi.org/10.1038/nature10361 PMID: 21772288
3. Tate CG, Schertler GF. Engineering G protein-coupled receptors to facilitate their structure determination. Curr Opin Struct Biol. 2009; 19(4):386–95. Epub 2009/08/18. https://doi.org/10.1016/j.sbi.2009.07.004 PMID: 19682887
4. Venkatakrishnan AJ, Deupi X, Lebon G, Tate CG, Schertler GF, Babu MM. Molecular signatures of G-protein-coupled receptors. Nature. 2013; 494(7436):185–94. Epub 2013/02/15. https://doi.org/10.1038/nature11896 PMID: 23407534
5. Venkatakrishnan AJ, Deupi X, Lebon G, Heydenreich FM, Flock T, Miljus T, et al. Diverse activation pathways in class A GPCRs converge near the G-protein-coupling region. Nature. 2016; 536(7617):484–7. https://doi.org/10.1038/nature19107 PMID: 27525504
6. Flock T, Ravarani CN, Sun D, Venkatakrishnan AJ, Kayikci M, Tate CG, et al. Universal allosteric mechanism for Galpha activation by GPCRs. Nature. 2015; 524(7564):173–9. Epub 2015/07/07. PubMed Central PMCID: PMC4866443. https://doi.org/10.1038/nature14663 PMID: 26147082
7. Warne T, Moukhametzianov R, Baker JG, Nehme R, Edwards PC, Leslie AG, et al. The structural basis for agonist and partial agonist action on a beta(1)-adrenergic receptor. Nature. 2011; 469(7329):241–4.

Epub 2011/01/14. PubMed Central PMCID: PMC3023143. https://doi.org/10.1038/nature09746 PMID: 21228877

8. Rosenbaum DM, Zhang C, Lyons JA, Holl R, Aragao D, Arlow DH, et al. Structure and function of an irreversible agonist-beta(2) adrenoceptor complex. Nature. 2011; 469(7329):236–40. Epub 2011/01/14. PubMed Central PMCID: PMC3074335. https://doi.org/10.1038/nature09665 PMID: 21228876
9. Zhang J, Zhang K, Gao ZG, Paoletta S, Zhang D, Han GW, et al. Agonist-bound structure of the human P2Y12 receptor. Nature. 2014; 509(7498):119–22. PubMed Central PMCID: PMCPMC4128917. https://doi.org/10.1038/nature13288 PMID: 24784220
10. Wang C, Jiang Y, Ma J, Wu H, Wacker D, Katritch V, et al. Structural basis for molecular recognition at serotonin receptors. Science. 2013; 340(6132):610–4. PubMed Central PMCID: PMCPMC3644373. https://doi.org/10.1126/science.1232807 PMID: 23519210
11. Lebon G, Warne T, Edwards PC, Bennett K, Langmead CJ, Leslie AG, et al. Agonist-bound adenosine A2A receptor structures reveal common features of GPCR activation. Nature. 2011; 474(7352):521–5. Epub 2011/05/20. PubMed Central PMCID: PMC3146096. https://doi.org/10.1038/nature10136 PMID: 21593763
12. Xu F, Wu H, Katritch V, Han GW, Jacobson KA, Gao ZG, et al. Structure of an agonist-bound human A2A adenosine receptor. Science. 2011; 332(6027):322–7. Epub 2011/03/12. PubMed Central PMCID: PMC3086811. https://doi.org/10.1126/science.1202793 PMID: 21393508
13. White JF, Noinaj N, Shibata Y, Love J, Kloss B, Xu F, et al. Structure of the agonist-bound neurotensin receptor. Nature. 2012; 490(7421):508–13. Epub 2012/10/12. PubMed Central PMCID: PMC3482300. https://doi.org/10.1038/nature11558 PMID: 23051748
14. Krumm BE, White JF, Shah P, Grisshammer R. Structural prerequisites for G-protein activation by the neurotensin receptor. Nat Commun. 2015; 6:7895. PubMed Central PMCID: PMCPMC4515772. https://doi.org/10.1038/ncomms8895 PMID: 26205105
15. Rasmussen SG, Choi HJ, Fung JJ, Pardon E, Casarosa P, Chae PS, et al. Structure of a nanobody-stabilized active state of the beta(2) adrenoceptor. Nature. 2011; 469(7329):175–80. Epub 2011/01/14. PubMed Central PMCID: PMC3058308. https://doi.org/10.1038/nature09648 PMID: 21228869
16. Choe HW, Kim YJ, Park JH, Morizumi T, Pai EF, Krauss N, et al. Crystal structure of metarhodopsin II. Nature. 2011; 471(7340):651–5. https://doi.org/10.1038/nature09789 PMID: 21389988
17. Standfuss J, Edwards PC, D'Antona A, Fransen M, Xie G, Oprian DD, et al. The structural basis of agonist-induced activation in constitutively active rhodopsin. Nature. 2011; 471(7340):656–60. https://doi.org/10.1038/nature09795 PMID: 21389983
18. Kruse AC, Ring AM, Manglik A, Hu J, Hu K, Eitel K, et al. Activation and allosteric modulation of a muscarinic acetylcholine receptor. Nature. 2013; 504(7478):101–6. PubMed Central PMCID: PMCPMC4020789. https://doi.org/10.1038/nature12735 PMID: 24256733
19. Sounier R, Mas C, Steyaert J, Laeremans T, Manglik A, Huang W, et al. Propagation of conformational changes during mu-opioid receptor activation. Nature. 2015; 524(7565):375–8. PubMed Central PMCID: PMCPMC4820006. https://doi.org/10.1038/nature14680 PMID: 26245377
20. Carpenter B, Nehme R, Warne T, Leslie AG, Tate CG. Structure of the adenosine A(2A) receptor bound to an engineered G protein. Nature. 2016; 536(7614):104–7. Epub 2016/07/28. PubMed Central PMCID: PMC4979997. https://doi.org/10.1038/nature18966 PMID: 27462812
21. Park JH, Scheerer P, Hofmann KP, Choe HW, Ernst OP. Crystal structure of the ligand-free G-protein-coupled receptor opsin. Nature. 2008; 454(7201):183–7. Epub 2008/06/20. https://doi.org/10.1038/nature07063 PMID: 18563085
22. Scheerer P, Park JH, Hildebrand PW, Kim YJ, Krauss N, Choe HW, et al. Crystal structure of opsin in its G-protein-interacting conformation. Nature. 2008; 455(7212):497–502. Epub 2008/09/27. https://doi.org/10.1038/nature07330 PMID: 18818650
23. Pardon E, Laeremans T, Triest S, Rasmussen SG, Wohlkonig A, Ruf A, et al. A general protocol for the generation of Nanobodies for structural biology. Nat Protoc. 2014; 9(3):674–93. PubMed Central PMCID: PMCPMC4297639. https://doi.org/10.1038/nprot.2014.039 PMID: 24577359
24. Carpenter B, Tate CG. Engineering a minimal G protein to facilitate crystallisation of G protein-coupled receptors in their active conformation. Protein engineering, design & selection: PEDS. 2016; 29 (12):583–94. Epub 2016/09/28.
25. Syrovatkina V, Alegre KO, Dey R, Huang XY. Regulation, Signaling, and Physiological Functions of G-Proteins. Journal of molecular biology. 2016; 428(19):3850–68. Epub 2016/08/16. PubMed Central PMCID: PMC5023507. https://doi.org/10.1016/j.jmb.2016.08.002 PMID: 27515397
26. Carpenter B, Tate CG. Expression, purification and crystallisation of the adenosine A2A receptor bound to an engineered mini-G protein. Bio-protocol; in press. 2017.

27. Warne T, Chirnside J, Schertler GF. Expression and purification of truncated, non-glycosylated turkey beta-adrenergic receptors for crystallization. Biochim Biophys Acta. 2003; 1610(1):133–40. PMID: 12586387

28. Warne T, Serrano-Vega MJ, Baker JG, Moukhametzianov R, Edwards PC, Henderson R, et al. Structure of a beta1-adrenergic G-protein-coupled receptor. Nature. 2008; 454(7203):486–91. Epub 2008/07/03. https://doi.org/10.1038/nature07101 PMID: 18594507

29. Thomas J, Tate CG. Quality control in eukaryotic membrane protein overproduction. J Mol Biol. 2014; 426(24):4139–54. PubMed Central PMCID: PMCPMC4271737. https://doi.org/10.1016/j.jmb.2014.10.012 PMID: 25454020

30. Carpenter B, Tate CG. Expression and purification of mini G Proteins from E. coli. Bio-protocol; in press. 2017.

31. Lebon G, Bennett K, Jazayeri A, Tate CG. Thermostabilisation of an agonist-bound conformation of the human adenosine A(2A) receptor. J Mol Biol. 2011; 409(3):298–310. https://doi.org/10.1016/j.jmb.2011.03.075 PMID: 21501622

32. Shibata Y, White JF, Serrano-Vega MJ, Magnani F, Aloia AL, Grisshammer R, et al. Thermostabilization of the neurotensin receptor NTS1. J Mol Biol. 2009; 390(2):262–77. Epub 2009/05/09. https://doi.org/10.1016/j.jmb.2009.04.068 PMID: 19422831

33. Chan P, Thomas CJ, Sprang SR, Tall GG. Molecular chaperoning function of Ric-8 is to fold nascent heterotrimeric G protein alpha subunits. Proc Natl Acad Sci U S A. 2013; 110(10):3794–9. PubMed Central PMCID: PMCPMC3593926. https://doi.org/10.1073/pnas.1220943110 PMID: 23431197

34. Green SA, Holt BD, Liggett SB. Beta 1- and beta 2-adrenergic receptors display subtype-selective coupling to Gs. Mol Pharmacol. 1992; 41(5):889–93. PMID: 1350321

35. Tate CG. A crystal clear solution for determining G-protein-coupled receptor structures. Trends in biochemical sciences. 2012; 37(9):343–52. https://doi.org/10.1016/j.tibs.2012.06.003 PMID: 22784935

36. Magnani F, Serrano-Vega MJ, Shibata Y, Abdul-Hussein S, Lebon G, Miller-Gallacher J, et al. A mutagenesis and screening strategy to generate optimally thermostabilized membrane proteins for structural studies. Nat Protoc. 2016; 11(8):1554–71. https://doi.org/10.1038/nprot.2016.088 PMID: 27466713

37. Zhang X, Stevens RC, Xu F. The importance of ligands for G protein-coupled receptor stability. Trends in biochemical sciences. 2015; 40(2):79–87. https://doi.org/10.1016/j.tibs.2014.12.005 PMID: 25601764

38. Lebon G, Warne T, Tate CG. Agonist-bound structures of G protein-coupled receptors. Curr Opin Struct Biol. 2012. Epub 2012/04/07.

39. Kawate T, Gouaux E. Fluorescence-detection size-exclusion chromatography for precrystallization screening of integral membrane proteins. Structure. 2006; 14(4):673–81. https://doi.org/10.1016/j.str.2006.01.013 PMID: 16615909

40. Kull B, Svenningsson P, Fredholm BB. Adenosine A(2A) receptors are colocalized with and activate g (olf) in rat striatum. Molecular pharmacology. 2000; 58(4):771–7. Epub 2000/09/22. PMID: 10999947

41. Chan P, Gabay M, Wright FA, Kan W, Oner SS, Lanier SM, et al. Purification of heterotrimeric G protein alpha subunits by GST-Ric-8 association: primary characterization of purified G alpha(olf). J Biol Chem. 2011; 286(4):2625–35. PubMed Central PMCID: PMCPMC3024758. https://doi.org/10.1074/jbc.M110.178897 PMID: 21115479

42. Serrano-Vega MJ, Tate CG. Transferability of thermostabilizing mutations between beta-adrenergic receptors. Mol Membr Biol. 2009; 26(8):385–96. Epub 2009/11/04. https://doi.org/10.3109/09687680903208239 PMID: 19883298

43. Hamm HE, Deretic D, Arendt A, Hargrave PA, Koenig B, Hofmann KP. Site of G protein binding to rhodopsin mapped with synthetic peptides from the alpha subunit. Science. 1988; 241(4867):832–5. Epub 1988/08/12. PMID: 3136547

44. Conklin BR, Farfel Z, Lustig KD, Julius D, Bourne HR. Substitution of three amino acids switches receptor specificity of Gq alpha to that of Gi alpha. Nature. 1993; 363(6426):274–6. Epub 1993/05/20. https://doi.org/10.1038/363274a0 PMID: 8387644

45. Conklin BR, Herzmark P, Ishida S, Voyno-Yasenetskaya TA, Sun Y, Farfel Z, et al. Carboxyl-terminal mutations of Gq alpha and Gs alpha that alter the fidelity of receptor activation. Mol Pharmacol. 1996; 50(4):885–90. Epub 1996/10/01. PMID: 8863834

46. Semack A, Sandhu M, Malik RU, Vaidehi N, Sivaramakrishnan S. Structural Elements in the Galphas and Galphaq C Termini That Mediate Selective G Protein-coupled Receptor (GPCR) Signaling. J Biol Chem. 2016; 291(34):17929–40. PubMed Central PMCID: PMCPMC5016181. https://doi.org/10.1074/jbc.M116.735720 PMID: 27330078

47. Nishimura A, Kitano K, Takasaki J, Taniguchi M, Mizuno N, Tago K, et al. Structural basis for the specific inhibition of heterotrimeric Gq protein by a small molecule. Proc Natl Acad Sci U S A. 2010; 107

(31):13666–71. PubMed Central PMCID: PMCPMC2922266. https://doi.org/10.1073/pnas.1003553107 PMID: 20639466

48. Tesmer VM, Kawano T, Shankaranarayanan A, Kozasa T, Tesmer JJ. Snapshot of activated G proteins at the membrane: the Galphaq-GRK2-Gbetagamma complex. Science. 2005; 310(5754):1686–90. https://doi.org/10.1126/science.1118890 PMID: 16339447

49. Clawges HM, Depree KM, Parker EM, Graber SG. Human 5-HT1 receptor subtypes exhibit distinct G protein coupling behaviors in membranes from Sf9 cells. Biochemistry. 1997; 36(42):12930–8. Epub 1997/10/23. https://doi.org/10.1021/bi970112b PMID: 9335552

50. Tate CG. Practical considerations of membrane protein instability during purification and crystallisation. Methods Mol Biol. 2010; 601:187–203. https://doi.org/10.1007/978-1-60761-344-2_12 PMID: 20099147

51. Oldham WM, Hamm HE. Structural basis of function in heterotrimeric G proteins. Q Rev Biophys. 2006; 39(2):117–66. https://doi.org/10.1017/S0033583506004306 PMID: 16923326

52. Wess J. G-protein-coupled receptors: molecular mechanisms involved in receptor activation and selectivity of G-protein recognition. FASEB J. 1997; 11(5):346–54. PMID: 9141501